

Chapter 11

Hypoxia Effects Within an Intra-guild Predation Food Web of *Mnemiopsis leidyi* Ctenophores, Larval Fish, and Copepods

Sarah E. Kolesar, Kenneth A. Rose and Denise L. Breitburg

Abstract Differences in predator and prey tolerances to abiotic factors, such as seasonal low dissolved oxygen (DO) concentrations in estuarine environments, can affect planktonic food web dynamics. Summertime hypoxia in the Chesapeake Bay alters field distributions, encounter rates, and predator–prey interactions between hypoxia-tolerant ctenophores, *Mnemiopsis leidyi*, and their less tolerant ichthyoplankton and zooplankton prey. Omnivory and intra-guild predation (IGP) increase the complexity of food webs, thereby confounding the effects of predation versus competition on prey populations. Omnivorous ctenophores in temperate estuarine food webs can both eat and compete with fish larvae for copepod prey. We isolated the effects of predation and competition, and how low versus high DO, affect larval fish growth and survival, using a spatially explicit (three vertical layers) individual-based model of a ctenophore–fish larvae–copepod IGP food web. We simulated three alternative food web structures of how ctenophores affect fish larvae (full interactions, relaxed predation, relaxed competition) under normoxic and hypoxic DO scenarios. Results from laboratory experiments and field studies were

S.E. Kolesar (✉)

Chesapeake Biological Laboratory, University of Maryland Center
for Environmental Science, 38 1 Williams Street, Solomons, MD 20688, USA
e-mail: sarah.kolesar@oregonstate.edu

Present Address:

S.E. Kolesar
Oregon Sea Grant, Oregon State University, 1600 SW Western Blvd.,
Corvallis, OR 97333, USA

K.A. Rose

Department of Oceanography and Coastal Sciences, Louisiana State University,
Energy, Coast, and Environment Building, Baton Rouge, LA 70803, USA

D.L. Breitburg

Academy of Natural Sciences Estuarine Research Center, 10545 Mackall Road,
St., Leonard, MD 20685, USA

Present Address:

D.L. Breitburg
Smithsonian Environmental Research Center, 647 Contees Wharf Road,
Edgewater, MD 21037, USA

used to configure and corroborate the model. Ctenophore predation had a bigger effect on survival of modeled fish larvae than did competition between ctenophores and fish larvae for shared zooplankton prey, but competition more strongly affected larval fish growth rates than did predation. Hypoxia versus normoxia did not alter the relative importance of ctenophore predation and competition, but low DO did decrease larval fish survival and increase larval growth rates. Model results suggest that consideration of the interaction strength in food webs and explicit treatment of spatial habitats to allow predator–prey overlap to emerge from movement will enhance our ability to predict hypoxia effects on fish.

Keywords Hypoxia · Bay anchovy · Fish eggs · Ichthyoplankton · Zooplankton · Predation · Trophic · Chesapeake Bay

11.1 Introduction

Hypoxia is increasing in coastal waters worldwide (Diaz and Rosenberg 2008; Gilbert et al. 2010; Rabalais et al. 2010; Zhang et al. 2010), with unknown but potentially meaningful effects on ecologically and commercially important species (Caddy 1993; Cloern 2001; Breitburg et al. 2009; Ekau et al. 2010; Levin et al. 2010). Hypoxia has well-documented effects on sessile species, and on the growth, survival, and reproduction of mobile individuals in localized areas. Furthermore, generalizations about hypoxia affecting mobile species at the population level are common (Kidwell et al. 2009 and references therein), although the quantitative evidence is mixed. Breitburg et al. (2009) did not find a strong relationship between fisheries landings and degree of hypoxia across coastal systems, but they caution that there are well-known problems with using landings data as indicators of population abundance. In a review of modeling analyses, Rose et al. (2009) determined that direct large-scale effects of hypoxia on coastal fish populations are relatively rare, but that there is potential for indirect effects of hypoxia on fish populations mediated via competitive and predation changes due to the responses of other members of the food web. Thus, examination of the effects of hypoxia within a food web context is appropriate, and may be necessary, to fully quantify hypoxia effects at the population level for key, mobile fish species.

Omnivory is common in many aquatic consumers and affects food web dynamics. Omnivory results in increased food web complexity that can dampen trophic cascades (Polis and Strong 1996; Snyder and Wise 2001) caused by strong top-down control in linear food chains. Feeding on multiple trophic levels disperses predation effects throughout the food web by creating weak trophic links (McCann et al. 1998). Trophic links are weaker when a predator is not wholly dependent upon any single resource for survival, such that the predator's actions may be more detrimental to the prey species than beneficial to the predator (Holt and Polis 1997;

Diehl and Fieel 2000). Omnivory also reduces the ability of predators to deplete any one trophic level in a system, and thus, omnivores are potentially less affected by food limitation than specialists. However, whether omnivores can limit the growth or abundance of competitors by depleting shared food resources is debatable (Polis and Strong 1996). The effect of omnivory on food webs is complicated, and it remains unclear whether the overall effect of omnivory is stabilizing or destabilizing (Fagan 1997; Vandermeer 2006).

Intraguild predation (IGP) is a specialized case of omnivory involving the consumption of one competitor by another, simultaneously conferring nutritional gain to the predator and eliminating a competitive rival (Polis et al. 1989). Intra-guild predation is widespread (Ehler 1996; Arim and Marquet 2004; Vandermeer 2006; Rosenheim 2007) and is particularly ubiquitous in marine and coastal systems (Polis et al. 1989; Thompson et al. 2007). Separating the indirect effects of competition from the direct effects of predation is challenging (Wissinger and McCrady 1993; Diehl 1995; Navarette et al. 2000). Understanding the role of omnivory, and especially IGP, in food web dynamics is important for predicting how coastal food webs will respond to hypoxia.

There are a variety of conditions under which the IGP form of omnivory can promote coexistence of the predator and prey species (i.e., increase food web stability). One of the most common situations is when the prey species is more efficient than the predator at utilizing the shared resource (Polis et al. 1989; Polis and Holt 1992; Holt and Polis 1997; Rosenheim 2007). Other situations that promote coexistence include: intermediate levels of disturbance (Gurevitch et al. 2000); seasonality in environmental conditions (Polis 1984); habitat structure (Janssen et al. 2007); intermediate levels of productivity (Diehl and Feiel 2000; Heithaus 2001); spatial refuges, temporal refuges, or resource subsidies that are unique to one of the species (Polis 1984; Wissinger 1992; Navarette et al. 2000; Amaraskare 2007); and age structure in which IGP-induced competition and predation differentially affects specific age classes (Polis 1984, 1998).

Our focus here is on a specific IGP food web (Chesapeake Bay) and how an IGP food web with different degrees of competition and predation interacts with low DO to affect food web responses. In the Chesapeake Bay and its tributaries such as the Patuxent River, a major component of the open-water food web involves ctenophores (*Mnemiopsis leidyi*), planktivorous fish larvae (e.g., bay anchovy, *Anchoa mitchilli*), and calanoid copepods (e.g., *Acartia tonsa*) (Fig. 11.1). Bay anchovy is an important forage fish species and the most abundant fish in the Chesapeake Bay system (Wang and Houde 1994). *Acartia tonsa* is the dominant summer crustacean mesozooplankton species in the mesohaline Chesapeake Bay (Brownlee and Jacobs 1987; Kimmel and Roman 2004). *Acartia* is consumed by both *M. leidyi* and larval bay anchovy, and *M. leidyi* also consumes larval bay anchovy. Similar food webs, with species substitutions, are found in many temperate coastal waters (Breitburg et al. 1997).

Low dissolved oxygen (DO) during the summer is a common feature in the main-stem Chesapeake Bay and also in many of its deep tributaries (Breitburg et al. 2003;

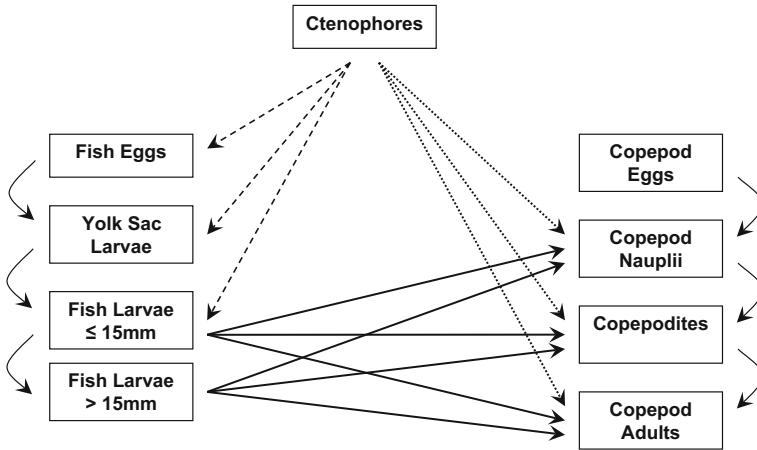


Fig. 11.1 Modeled mesohaline summertime Chesapeake Bay system food web. The food web includes intra-guild predation (IGP) with ctenophores as the intra-guild predators (IG predators) feeding on both the early life stages of fish (eggs, yolk sac larvae, and feeding larvae ≤ 15 mm) and three copepod life stages (nauplii, copepodites, and adults). Straight arrows represent influence of predator on prey. Transitions from one life stage to the next are indicated with curved arrows. The relaxed predation model scenario eliminates ctenophores feeding on the early life stages of fish (*dashed lines*), and the relaxed competition scenario reduces ctenophore feeding on the three copepod life stages (*dotted lines*). Larval fish ≤ 15 mm are the IG prey

Kemp et al. 2005) and can affect the stability of the IGP food web by differentially affecting the vertical distributions of the species. Field studies indicate that low DO concentrations can cause behavioral responses in habitat use and distribution by motile organisms such as *Mnemiopsis leidyi*, fish larvae, and zooplankton (Breitburg et al. 2003; Kolesar et al. 2010). Field data demonstrated how increased habitat overlap between ctenophores and copepods in a stratified water column led to elevated predation rates, especially near the pycnocline (Purcell et al. 2014). Indeed, increasing hypoxia has been associated with shifts in estuarine food webs to greater domination by jellyfish (Purcell et al. 2001).

In this paper, we used an individual-based simulation model to examine the roles of predation, competition, and low DO in the *M. leidyi*-fish larvae-copepod intra-guild food web. The model simulates predation by *M. leidyi* on fish larvae and zooplankton, and predation by fish larvae on zooplankton, in a three-layer water column for the summer months using information representative of the mesohaline portion of the Patuxent River. Simulations were performed to quantify the effects of low DO on food web dynamics and to isolate the effects of competition versus predation on larval fish growth and survival by *M. leidyi*. Our modeling results provide a basis for determining whether hypoxia effects in this common estuarine food web are general or are highly dependent on the relative strengths of competition and predation, which can vary over time within a system and among systems.

11.2 Model Description

11.2.1 Overview

The model follows the growth, mortality, and movement of *Mnemiopsis leidyi* ctenophores, fish larvae, and copepods every 12 h (day and night time steps) for the summer months in a three-layer water column. Temperature was assumed constant throughout the simulation, and dissolved oxygen (DO) concentrations varied over time in each of the three layers. Ctenophores and fish larvae were followed as individuals; copepods were followed as the numbers in each of three uncoupled life stages (nauplii, copepodites, and adults). Fish larvae were introduced as daily cohorts of eggs, while the net energy consumed by adult ctenophores determined the production of new ctenophores. Fish eggs and yolk sac larvae, and eggs and larvae of ctenophores, were followed using matrix projection models. The survivors to the end of the larval stages in the two matrix models (fish, ctenophores) were then treated as individuals in the simulation. Growth of individual ctenophores and fish larvae was based on similarly formulated bioenergetics models with consumption dependent on their encounters with their prey. Ctenophores ate copepods and fish larvae, and fish larvae ate copepods. Mortality of ctenophores was assumed to be constant; mortality of fish larvae and copepods included predation by other modeled individuals. Dissolved oxygen determined movement of ctenophores and fish larvae among the layers and directly affected mortality of fish eggs and growth rates of ctenophores and fish larvae. All variables used in model equations are defined in Table 11.1.

11.2.2 Water Column Structure

The simulated water column was configured to be representative of the summertime conditions typical of the deep, mesohaline region of the Patuxent River that experiences summertime hypoxia. The water column is 1 m × 1 m × 20 m deep and divided into three layers with 20% of the volume in the surface layer, 30% in the pycnocline layer, and 50% in the bottom layer. Two DO conditions were simulated: well mixed with DO concentrations of 6.0 mg L⁻¹ in all three layers (high or normoxic) and stratified with surface, pycnocline, and bottom DO set to 6.0, 3.0, and 1.5 mg L⁻¹ (low or hypoxic), respectively. The DO concentration of 1.5 mg L⁻¹ is typical for summer conditions and is sufficiently low to alter vertical distributions of organisms (Breitburg et al. 2003) and affect predator-prey interactions (Decker et al. 2004), causing maximum overlap between ctenophores and their prey at or near the pycnocline (fish larvae and copepods avoid DO <2 mg L⁻¹). Temperature conditions were held constant at 24 °C in all layers for the duration of the simulations.

Table 11.1 Variable names, descriptions, and units used in the individual-based model

Variable	Description	Units
<i>LvWt</i>	Larval fish weight	mg dw
<i>LvLn</i>	Larval fish length	mm
<i>CtWt</i>	Ctenophore weight	mg dw
<i>CtLn</i>	Ctenophore length	mm
<i>LvCap</i>	Vulnerability of zooplankton prey to larval fish predators based on prey type and larval fish length	Proportion
<i>LvCon</i>	Larval fish consumption	mg dw 12 h ⁻¹
<i>LvAsm</i>	Larval fish assimilation	Fraction
<i>LvRsp</i>	Larval fish total respiration per time step	mg dw 12 h ⁻¹
<i>j</i>	Prey type (fish egg, yolk sac, or copepod life stage)	–
<i>i</i>	Water column layer (surface, pycnocline, bottom)	–
<i>t</i>	Time	h
<i>LvCmax</i>	Fish larvae maximum consumption	mg dw 12 h ⁻¹
<i>ZZ</i>	Number of each zooplankton prey type	Number m ⁻³
<i>T</i>	Temperature in the water column layer	°C
<i>KK</i>	Half-saturation parameter for larval functional response	Number m ⁻³
<i>ZpWt</i>	Copepod weight	mg dw
<i>LvRRsp</i>	Larval fish routine respiration per time step at 24 °C	mg dw 12 h ⁻¹
<i>CtCon</i>	Ctenophore consumption	mg dw 12 h ⁻¹
<i>CtAsm</i>	Ctenophore assimilation	Fraction
<i>CtRsp</i>	Ctenophore respiration	mg dw 12 h ⁻¹
<i>CtRpr</i>	Fraction of net energy intake used for reproduction by ctenophore	Fraction
<i>Fpp</i>	Ctenophore foraging rate	mm 12 h ⁻¹
<i>Fpred</i>	Foraging rate used if ctenophore distance swum is greater	mm 12 h ⁻¹
<i>Fprey</i>	Foraging rate used if larval fish distance swum is greater	mm 12 h ⁻¹
<i>DsPred</i>	Distance swum by the predator	mm 12 h ⁻¹
<i>DsPrey</i>	Distance swum by the prey	mm 12 h ⁻¹
<i>CtRd</i>	Ctenophore reactive distance	mm
<i>PrRd</i>	Prey reactive distance	mm
<i>E</i>	Mean numbers of encounters	Number 12 h ⁻¹ m ⁻³
<i>PD</i>	Number of prey available for encounter per layer	Number m ⁻³
<i>CtCapLv</i>	Ctenophore capture success of individual fish larvae	Fraction
<i>CtConCal</i>	Ctenophore consumption	Calories
<i>CtRprCal</i>	Calories available for ctenophore reproduction	Calories

(continued)

Table 11.1 (continued)

Variable	Description	Units
<i>ZProd</i>	Copepod production rate	12 h ⁻¹
<i>TotZ</i>	Copepod maximum density	Number m ⁻³
<i>Vol</i>	Water column volume	m ⁻³
<i>DO</i>	Dissolved oxygen concentration	mg L ⁻¹
<i>SurvEggDO</i>	Fish egg survival due to DO	Number 12 h ⁻¹
<i>CtWorth</i>	Modeled superindividual ctenophore	Number
<i>LvWorth</i>	Modeled superindividual larval fish	Number

11.2.3 Larval Fish—Energetics and Consumption

Fish eggs were introduced into the surface layer at the beginning of the nighttime step at a density of 100 m⁻³, and the abundances of fish eggs and yolk sac larvae (total number) in each layer every 12 h were simulated using two-stage matrix projection models that were specific to each layer (Appendix A). Eggs were introduced every 3 days beginning in early June (day 150), increased to daily during July (days 190–212), and then decreased to every 3 days until August (day 220). The elements of the matrix models for each layer were determined every 12 h, and numbers of individuals in each stage in each layer were updated including the addition of newly spawned eggs and ctenophore consumption included as mortality. The number of exiting yolk sac larvae (entering the feeding larvae stage) on each day was lumped over layers and subsequently followed as individual larvae. All new larval individuals were started at 3 mm (0.0084 mg dw) and in the bottom layer. No direct egg cannibalism was assumed. Fish eggs and larvae in the model were mostly based upon information about bay anchovy.

Individual larvae grew according to a bioenergetics equation with consumption based on density-dependent encounter rate of predator and zooplankton prey. Larval fish weight was incremented each 12 h based on consumption (*LvCon*, mg dw 12 h⁻¹, day time step only), assimilation (*LvAsm*, fraction), and respiration (*LvRsp*, mg dw 12 h⁻¹):

$$LvWt_t = LvWt_{t-1} + LvCon \cdot LvAsm - LvRsp \quad (11.1)$$

Larval length (*LvLn*) was then determined from weight (*LvWt*) using a length–weight relationship. Weight was allowed to increase or decrease each time step, but length was not allowed to shrink. A new length was computed if the individual was at the weight expected for its length and if the change in weight was positive.

Larval fish consumption, assimilation, and respiration were based on larval weight, temperature, and prey densities (Adamack et al. 2012; Rose et al. 1999). Maximum consumption was dependent on larval weight, and a constant temperature of 24 °C was assumed ($LvCmax = a \cdot LvWt^b$, if *LvWt* weight < 0.022,

$a = 27.71$, $b = 0.76$; if $LvWt \geq 0.022$, $a = 28.87$, $b = 0.75$) and was used with a multi-species type II functional response relationship to determine realized consumption of each of the three zooplankton types (nauplii, copepodites, adults):

$$LvCon_j = LvCmax \cdot \frac{ZZ_j}{Vol} \cdot \frac{\frac{LvCap_j}{KK_j}}{1 + \sum_i^3 \frac{LvCap_i}{KK_i} \cdot ZpWt_i} \cdot ZpWt_j \quad (11.2)$$

where $LvCon_j$ is realized cumulative consumption rate of the j th zooplankton type ($\text{mg dw } 12 \text{ h}^{-1}$), $LvCap$ is the vulnerability of zooplankton prey to larval fish predators based on prey type and larval fish length (after Rose et al. 1999; maximum $LvCap_j = 0.9$), ZZ_j is density of zooplankton type j (number m^{-3}), KK_j is the half-saturation parameter of the larval fish for zooplankton type j , and $ZpWt_j$ is the weight per individual (mg dw) of zooplankton type j . Vol is the volume of the layer (m^3). The sum of the three zooplankton-type specific consumption rates is the total

12-h consumption rate for the larva in Eq. 11.1 (i.e., $LvCon = \sum_{j=1}^3 LvCon_j$). The KK_j

were calibrated to obtain realistic larval fish growth rates (Table 11.2). Feeding occurred only during daytime time steps. Assimilation efficiency ($LvAsm$) was set at 0.60 (Rose et al. 1999). Respiration ($LvRRsp$) was computed as a routine rate

Table 11.2 Values used for modeled organism weight, energy density, and length. Individual larval fish and ctenophore weight and length varied with consumption during model simulations. Fish egg and yolk sac larvae weights were based on values reported in Tucker (1989). Energy densities of all fish life stages were based on values from Hunter and Leong (1981). Ctenophore energy density values were reported in Harris et al. (2000). Energies densities for all copepod life stages were reported in Laurence (1976) and weights as reported in Tester and Turner (1988). Fish eggs, yolk sac larvae, and zooplankton lengths were estimated from live samples. Larval fish consumption was modeled using a multi-species type II functional response, and realized consumption for each prey type was estimated by applying KK , the half-saturation parameter, to prey densities in the model

	Weight per individual (mg dw)	Energy density (calories mg dw ⁻¹)	Length per individual (mm)	Calibrated KK values (number m ⁻³)
Fish eggs	0.00842	5.525	1	NA
Yolk sac larvae	0.015	5.424	3	NA
Fish larvae	Dynamic	5.350	Dynamic	NA
Ctenophores	Dynamic	2.967	Dynamic	NA
Nauplii	0.00152	5.160	0.15	75,000
Copepodites	0.0033	5.160	0.6	3000
Adult copepods	0.011	5.160	1.2	2250

dependent upon larval weight ($LvWt$) and a constant water temperature ($T = 24$ °C) for nighttime and twice the routine rate for daytime. The routine rate was:

$$LvRRsp = 0.073 \cdot LvWt^{0.997} e^{\frac{\log(2.2)}{10} \cdot (T-27)} \quad (11.3)$$

Individual fish larvae died from being eaten by ctenophores and from a constant rate representative of mortality from other sources. Mortality rate was set to 3% per 12 h to reflect predation by *Chrysaora quinquecirrha* medusae and piscivorous fish (Cowan and Houde 1993; Purcell et al. 1994a; Purcell and Arai 2001). Larger larval fish (≥ 15 mm) were no longer vulnerable to ctenophore predation, but were kept in the simulation to include their consumption effects on zooplankton prey.

11.2.4 Ctenophores—General Bioenergetics

The model assumed that ctenophores could potentially produce eggs every 12 h based on their consumption rate. As with fish eggs and yolk sac larvae, the numbers of ctenophore eggs and larvae in each layer were tracked using a two-stage matrix projection model for each layer (Appendix A). The mortality rates of ctenophore eggs and larvae used in the matrix model were determined by calibration to generate reasonable ctenophore and fish larval densities in simulations. Individuals exiting the larval stage entered an intermediate holding stage (prereproductive lobate stage) where they waited until reaching 25 mm length (another 5–7 days, depending on growth rates) and entered the model as individual reproductive ctenophores in the layer they were spawned in.

Similar bioenergetics as with fish larvae, with the addition of reproduction costs, was also used for the 25 mm and longer individual ctenophores:

$$CtWt_t = CtWt_{t-1} + (CtCon \cdot CtAsm - CtRsp) \cdot (1 - CtRpr) \quad (11.4)$$

where $CtWt$ is weight of a ctenophore (mg dw), $CtCon$ is the consumption rate (mg dw 12 h^{-1}), $CtAsm$ is assimilation (fraction), $CtRsp$ is respiration rate (mg dw 12 h^{-1}), and $CtRpr$ is fraction of net energy intake used for reproduction. Ctenophore length ($CtLn$; mm) was determined from weight ($CtWt$) using a length–weight relationship (Kremer 1976).

Consumption was based on a modified version of the Gerritsen and Strickler (1977) encounter model (Cowan et al. 1999; Kolesar 2006). Ctenophores fed during both day and night time steps on fish eggs, yolk sac larvae, fish larvae (≤ 15 mm), and the three stages of copepods. Encounters were dependent on swimming speeds and encounter radii of the ctenophores and each of their prey types, both of which were dependent on body length (BL; mm). Capture success was fixed for smaller, less motile prey and varied with length for larval fish prey.

11.2.5 *Ctenophores—Encounters, Consumption, and Energetics*

Ctenophores and fish larvae had dynamic individual lengths that varied based on their bioenergetics and growth; fixed lengths were used for eggs, yolk sac larvae, and copepods (Table 11.2). Swimming speeds were assumed to be 0.3 BL s^{-1} for ctenophores (Kolesar 2006), and 2 BL s^{-1} for yolk sac larvae, feeding larvae, and copepods; fish eggs were assumed not to swim. Reactive distance of ctenophores ($CtRd$, mm) was based on their length (mm) and modeled as an ellipse:

$$CtRd = 0.5 \cdot \left(0.33 \cdot CtLn + \frac{0.33 \cdot CtLn}{2} \right) \quad (11.5)$$

Reactive distances for all prey types ($PrRd$, mm) were assumed to be their length in mm.

By combining swimming speeds and reactive distances with prey density, we computed the mean number of encounters (E) in 12 h (number $12 \text{ h}^{-1} \text{ m}^{-3}$) between a ctenophore predator and each of its prey types:

$$E_j = \pi \cdot (PrRd_j + CtRd)^2 \cdot Fpp_j \cdot 10^{-9} \cdot PD_j \quad (11.6)$$

where $PrRd_j$ is encounter radius of prey type j (mm), $CtRd$ is the encounter radius of the ctenophore (mm), Fpp_j is the foraging rate ($\text{mm } 12 \text{ h}^{-1}$) of the ctenophore and prey type j , and PD_j is density (number m^{-3}) of prey type j . In Eq. 11.6, there were six possible prey types: fish eggs, yolk sac larvae, fish larvae, and the three stages of the copepods. The foraging rate depended on the distances swum by the predator ($DsPred$, mm) and prey type j ($DsPrey_j$, mm) in 12 h:

$$Fpp_j = \begin{cases} Fpred & \text{if } DsPred > DsPrey_j \\ Fprey & \text{if } DsPred \leq DsPrey_j \end{cases} \quad (11.7)$$

where

$$Fpred = \frac{(DsPrey_j^2 + 3 \cdot DsPred^2)}{3 \cdot DsPred}$$

$$Fprey = \frac{(DsPred^2 + 3 \cdot DsPrey_j^2)}{3 \cdot DsPrey_j}$$

Prey density (PD_j , number m^{-3}) for copepods, fish eggs, and yolk sac larvae was the total number in each layer divided by the volume of that layer. For fish larvae, which were followed as individuals, Eq. 11.6 was evaluated for each individual fish larva as a possible prey item for each ctenophore.

For each ctenophore and prey type, the number of prey of each type encountered and captured was multiplied by weight per individual, adjusted for energy density (calories per mg dw, Table 11.2), and summed to obtain biomass eaten by the ctenophore ($CtCon$ in Eq. 11.4). Realized number of encounters was generated as a random deviate from a Poisson distribution with mean equal to E_j . The actual number of prey encountered and successfully captured was then determined as a deviate from a binomial distribution with the number of trials equal to the number of realized encounters (Poisson deviate generated from E_j) and the probability of success set to the probability of capture. Capture success by ctenophores was 0.62 for nauplii, 0.54 for copepodites, and 0.46 for adults (Waggett and Costello 1999), and 0.80 for fish eggs and yolk sac larvae (Cowan and Houde 1993). Capture success for ctenophore feeding on individual fish larvae ($CtCapLv$) depended on the lengths (mm) of both predator and prey and was not allowed to exceed 0.80 (Cowan and Houde 1993; Kolesar 2006):

$$CtCapLv = 1.086 - 6.99 \cdot \frac{LvLn}{CtLn} \quad (11.8)$$

Biomass eaten of prey type was computed from actual numbers eaten and the weight (mg dw) per individual prey item (Table 11.2), and then converted to calories (Table 11.2) and summed to obtain total consumption in calories for the ctenophore. This total consumption was then divided by the energy density of the ctenophore to obtain prey consumption back in units of mg dw, but now in terms of ctenophore tissue. We adjusted prey consumed by ctenophores by energy densities because energy densities of ctenophores were about half of their prey.

Based on data reported in Kremer (1976, 1979), Kremer and Reeve (1989), and Reeve et al. (1989), we fit a logistic-shaped function that relates assimilation efficiency ($CtAsm$) to prey consumption (Fig. 11.2); assimilation efficiency ranged from a maximum of 0.9 at low food densities to a minimum of 0.4 at the highest prey densities.

Respiration ($CtRsp$) depended on weight and was modified from Kremer (1976) for the 24 °C and 12 h time step used in this model:

$$CtRsp = 4.4 \cdot e^{0.15 \cdot T} \cdot 7.06 \times 10^{-4} \cdot 1.67 \cdot 0.5 \cdot CtWt \cdot 0.5 \quad (11.9)$$

where 7.06×10^{-4} converts $(\mu\text{M CO}_2) \cdot \text{g dw}^{-1}$ to $\text{g dw} \cdot (\mu\text{M C})^{-1}$, 1.67 converts $\text{g dw} \cdot (\mu\text{M C})^{-1}$ to the total daily fraction of body carbon catabolized; the first 0.5 value adjusts the rate for the warmer temperature of the Patuxent River, and the second 0.5 value converts the daily rate to a rate per 12 h.

Net energy consumed was divided between somatic growth and reproduction. Maturity occurred at 25 mm (Reeve et al. 1989). Immature individuals used all of their net energy for growth, while mature individuals allocated up to 100% of their net energy to egg production. On each nighttime time step, the proportion of net energy allocated to reproduction ($CtRpr$) was calculated (Kremer 1976):

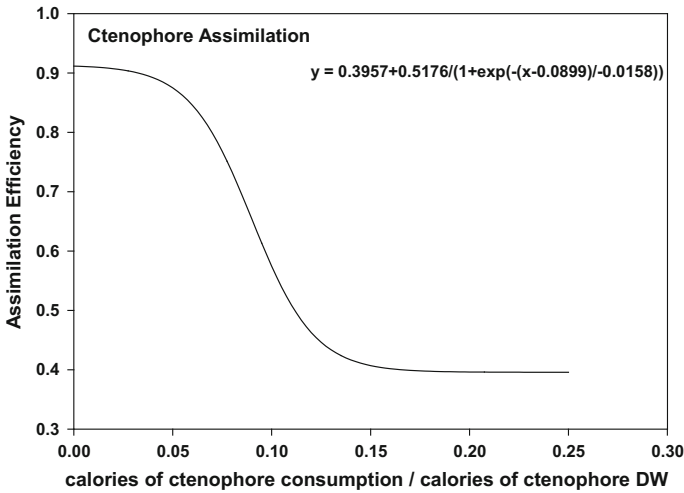


Fig. 11.2 Equation for ctenophore assimilation efficiency used in the model determined from published data on ctenophore assimilation as well as information on ctenophore bioenergetics (consumption based on biomass)

$$CtRpr = 0.01 \cdot e^{0.115 \cdot CtWi} \quad (11.10)$$

Net energy gain (i.e., $CtCon \cdot CtAsm - CtRsp$, in mg dw) was summed for the day (daytime plus nighttime; eggs were released at night) and converted to calories based on the energy densities and biomasses eaten of the prey in the diet comprising $CtCon$, and respiration rate was converted to calories ($CtRsp \cdot 2.967$). Net energy gain in calories was then multiplied by $CtRpr$ to obtain energy (in calories) available for eggs, and this was done for the day and night time steps and summed to obtain a single daily value ($CtRprCal$). The daily value was used to determine the number of eggs produced by that ctenophore for that day (Grove and Breitbart 2005):

$$CtEgg = 647.5 \cdot \log(CtRprCal) + 926.75 \quad (11.11)$$

Mortality of ctenophores was $5\% \text{ } 12 \text{ h}^{-1}$ for before August 1 and $15\% \text{ } 12 \text{ h}^{-1}$ after August 1 (day 213). *Chrysaora quinquecirrha* and *Beroe ovata* ctenophores that consume *M. leidy* typically peak in mid- to late summer (Kreps et al. 1997; Purcell et al. 2001).

11.2.6 Copepods

The numbers of individuals in each of the three life stages of the copepods (nauplii, copepodites, and adults) in each layer were simulated separately using a logistic

production model with added mortality terms based on the summed consumption from individual ctenophores and the summed consumption from individual larvae.

$$ZZ_{j,t} = ZZ_{j,t-1} + ZProd_j \cdot \left(1 - \frac{ZZ_{j,t-1}}{TotZ_j} \right) - \sum_{i=1}^n \frac{LvCon_{i,t-1}}{Vol} - \sum_{k=1}^m \frac{CtCon_{k,t-1}}{Vol} \quad (11.12)$$

where $ZZ_{j,t}$ is the number of each copepod life stage j in the model in a layer at time t , $Zprod_j$ is the production rate (12 h^{-1}) of zooplankton type j , $TotZ_j$ is the maximum density (number m^{-3}) of type j , n is the number of larvae in the layer, and m is the number of ctenophores in the layer. $Zprod_j$ was set to 0.6, 0.5, and 0.4, and $TotZ$ was set to 300,000 nauplii, 15,000 copepodites, and 10,000 adults.

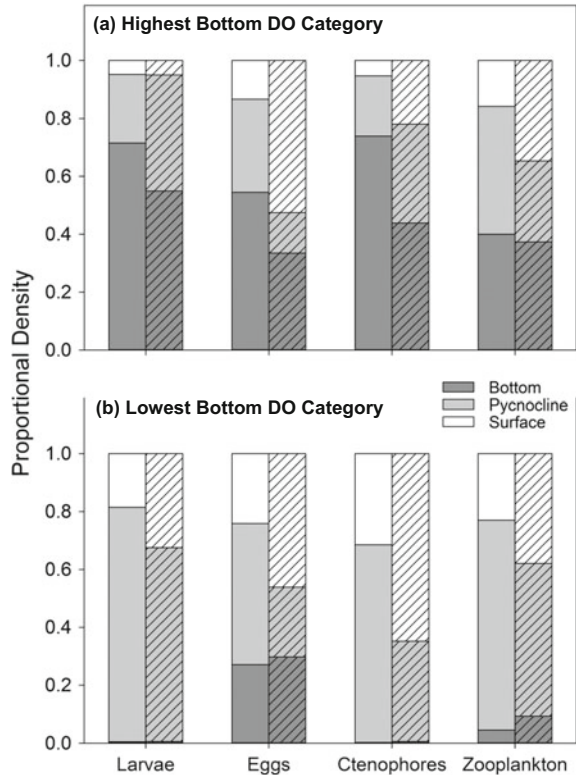
11.2.7 Vertical Movement of Fish, Ctenophores, and Copepods

Movement of fish egg densities, yolk sac larval densities, copepod densities, and individual model fish larvae and ctenophores occurred every time step in the simulation. Modeled movement among the three water column layers was based on the proportional densities of organisms, dependent on bottom layer DO concentration (similar calculations found in Breitburg et al. 2003; Keister et al. 2000; Kolesar et al. 2010). Proportional densities of organisms were calculated for a water column, assuming equal volumes of water in all three layers, and for discrete intervals of DO (two interval scenarios are shown in Fig. 11.3). We linearly interpolated from proportional densities by DO interval to the modeled proportional densities for high DO conditions (6.0 mg L^{-1} in all three layers) and for low DO conditions (6.0 mg L^{-1} in the surface layer, 3.0 mg L^{-1} in the pycnocline layer, and 1.5 mg L^{-1} in the bottom layer), and adjusted the proportional densities for the unequal volumes of the three layers by multiplying by the volume of each layer. We then formed the cumulative distribution of these interpolated, volume-adjusted proportions and generated a random number between 0 and 1 every 12 h to determine the fraction of the individuals (eggs, yolk sac, copepods) or the probability an individual (larvae and ctenophores) would move for the next time step. Separate proportional densities by bottom DO were used for fish eggs and for fish larvae and the proportional densities of larval fish were also used for yolk sac larvae.

11.2.8 Dissolved Oxygen Effects

In addition to vertical movement, low DO directly affected larval fish growth, ctenophore growth, and fish egg survival. We combined laboratory results for

Fig. 11.3 Proportional densities of fish larvae, eggs, ctenophores, and zooplankton. Distribution of each organism type was calculated for an idealized water column with equal water volume in surface (white), pycnocline (light gray), and bottom (dark gray) layers during the day (unhatched bars) and night (hatched bars) for two bottom dissolved oxygen (DO, mg L⁻¹) categories, **a** highest bottom layer DO category (6–6.99 mg L⁻¹) and **b** lowest bottom layer DO category (1–1.99 mg L⁻¹)



anchovy and naked goby (Zastrow et al. unpubl.) to develop a multiplier of growth rate due to low DO:

$$GrLvDO = -0.00397 + 0.482 \cdot DO^{0.389} \tag{11.13}$$

On each time step, the DO in the layer was used to determine *GrLvDO*, which was then multiplied by the growth rate according to bioenergetics (Eq. 11.1) and the adjusted growth rate was used to increment larval fish weight. The same approach was used to modify ctenophore growth (Grove and Breitburg 2005):

$$GrCtDO = \frac{0.1173 + 0.0104 \cdot DO}{0.1797} \tag{11.14}$$

Fish egg survival under low DO was based on Dorsey et al. (1996):

$$SurEggDO = \frac{95.77}{1 + e^{\frac{2.35 - DO}{0.95}}} \tag{11.15}$$

Fraction of eggs surviving 12 h used in the stage-based matrix model for fish eggs and yolk sac larvae were multiplied by *SurEggDO* based on the DO in the layer (Appendix A).

11.2.9 Numerical Considerations

We used a superindividual approach for representing ctenophore and larval fish model individuals. The superindividual approach allows for a predetermined number of model individuals to be in a simulation, thereby preventing numerical coding problems associated with following thousands or millions of model individuals (Scheffer et al. 1995). In our model, ctenophore reproduction was simulated based on energy consumed. However, adding a new model individual for every new ctenophore introduced into the model could result in the computer code exceeding memory limitations. The superindividual approach addresses this by making each model individual worth some number of identical population individuals. Thus, a known number of model individuals can be added and their worth adjusted to reflect the population number added. Mortality is then simulated by decrementing the worth of the superindividual to reflect the loss of population individuals represented by the superindividual. In all model simulations, five ctenophore superindividuals and five larval fish superindividuals were introduced into each layer at the start of every time step. The worth of ctenophore superindividuals (*CtWorth*) and larval fish superindividuals (*LvWorth*) was calculated by dividing the number of population individuals of one type introduced into each layer at each time step by 5, and assigning that same worth to each superindividual.

Mortality and predation were imposed on ctenophore and fish larvae superindividuals by adjusting the population worth of each superindividual. Mortality, either as a fixed mortality rate on either ctenophore or larval fish, or by ctenophore predation on a larval fish, resulted in a reduction of the population worth of the superindividual. Because the ctenophores (predator) and larval fish (prey) were both superindividuals, when a model ctenophore ate one or more of the population individuals of a model fish larva, we had to make adjustments to ensure mass balance. If the ctenophore worth times the number of population larvae it ate was less than the worth of the larval superindividual, then the ctenophore individual consumed the entire weight of the larval individual. The model ctenophore grew accordingly, and the larval worth was reduced by the worth of the ctenophore superindividual times the number of larvae eaten. If the ctenophore worth times the number of population larvae it ate was greater than the worth of the larval superindividual, then the ctenophore actually consumed the weight of the larval fish times the ratio of larval worth to ctenophore worth and the worth of the larva superindividual was set to 0. In this way, mass balance of the biomasses of ctenophores and fish larvae was maintained.

Ctenophore predation on larval fish and copepods, and larval fish predation on copepods, was updated after each ctenophore and larval fish evaluation as the predator. This was done to minimize the possibility of summed predation pressure over ctenophores or fish larvae exceeding the prey abundance in a layer on a time step. Because we updated the larval fish worths and copepod densities for predation after every predator, each time step the ctenophores and larval fish individuals were evaluated for growth and mortality in random order. Otherwise, modeled individuals evaluated first would always see higher prey densities.

Predation by ctenophores on fish eggs and yolk sac larvae was accounted for by the dynamic mortality term included in the estimation of the diagonal and subdiagonal terms of their stage-based matrix projection model. Predation by ctenophores and larval fish on each of the three copepods stages was accounted for by inclusion of the mortality rate in each logistic production equation.

11.3 Design of Model Simulations

All model simulations were for 100 d from May 25 (day 145) to September 2 (day 245). Five replicate simulations were performed for each condition using different random number sequences that affected encounter rates, capture success, and movement. The model was first calibrated and corroborated under baseline conditions. Baseline conditions included the full IGP food web: ctenophore consumption caused mortality of fish larvae, and ctenophore and fish larval consumption caused mortality of copepods. We then used the calibrated model to explore how predation, competition, and hypoxia effects interact to affect food web dynamics. Because model predictions were very similar among replicates (see minimum and maximum values in Table 11.3), we focus on the output variables averaged over the five replicates and graph results (e.g., time series plots, diets) from one replicate simulation.

11.3.1 Calibration and Corroboration

We adjusted several key parameters in the baseline model under both high and low DO conditions to obtain realistic model behavior compared to field data. The KK_j in Eq. (11.2) were adjusted to obtain realistic larval fish growth rates, and then the fixed mortality rates of fish and ctenophore eggs and larvae were adjusted to generate reasonable summertime averaged fish densities and ctenophore densities. The high DO (normoxic, 6.0 mg L⁻¹ in all layers) and low DO (hypoxic, 6.0, 3.0, and 1.5 mg L⁻¹) simulations were used because the field data reflect a range of DO conditions. We first crudely compared larval fish growth rates and ctenophore

Table 11.3 Comparison of simulated densities of ctenophores, fish eggs, yolk sac larvae, post-yolk sac (feeding) larvae, copepod nauplii, copepodites, and adult copepods with reported field densities (all m^{-3}). Model values presented are the mean \pm SE, and minimum and maximum, of the 100 daily densities entering each life stage. Each value for the field data was a summertime mean based on the available stations and sampling dates. There were generally 43 stations for the Patuxent sampling and 174 stations for the Chesapeake Bay sampling for ctenophores and fish; about 15 stations for zooplankton sampling. Field densities of ctenophores and fish were measured in the Chesapeake Bay in July and August 1995–1998 (data from the TIES project, summarized in Purcell et al. 2001, Tables 6 and 7) and the Patuxent River in June, July, and August 1992, 1993, 1999, and 2001 (Keister et al. 2000; Breitbart et al. 2003; Kolesar et al. 2010). Copepod nauplii, copepodite, and adult copepod field densities were from June, July, and August of 2000 and July 2001 for the Chesapeake Bay and from June, July, and August of 1999 and July 2001 for the Patuxent River in (Purcell et al. 2014 and unpublished data). For the field data, yolk sac larvae and feeding larval fish densities were combined and are reported under (fish larvae), and copepodite and adult copepod densities were combined (copepods). Ctenophore and fish data are presented for the whole water column; copepod data are presented for the surface layer only. Copepods are presented as thousands m^{-3}

	Model results		Field data	
	High DO	Low DO	Patuxent	Chesapeake Bay
Ctenophores	3.8 \pm 0.2 (0.01–8.7)	3.7 \pm 0.2 (0.02–7.9)	0.03–6.83	2.8–12.7
Fish eggs	2.5 \pm 0.5 (0–20)	2.7 \pm 0.5 (0–20)	0–41.3	1.2–28.8
Yolk sac larvae	1.4 \pm 0.2 (0–10)	0.5 \pm 0.1 (0–4)		
Fish larvae	1.5 \pm 0.1 (0–6)	0.6 \pm 0.03 (0–2.3)		
Yolk sac plus larvae			1.6–12.9	0.3–3.3
Nauplii	226.9 \pm 7.4 (92.1–399.6)	190.8 \pm 6.1 (66.5–393.6)	36.4–38.3	20.4–27.7
Copepodites	10.6 \pm 0.4 (3.7–10.0)	8.7 \pm 3.3 (2.6–19.7)		
Adult copepods	6.3 \pm 0.3 (1.6–13.3)	4.9 \pm 0.3 (1.0–13.1)		
Copepodites plus adult copepods			0.7–29.5	0.8–7.5

lengths and egg production rates to values reported in the literature. We then compared averaged densities of fish eggs, yolk sac plus larvae, ctenophores, and copepods (nauplii and copepodites plus adults), computed over a single replicate simulation for high and low DO conditions to field-measured densities for the Patuxent River estuary and Chesapeake Bay.

11.3.2 Predation, Competition, and DO Effects Within the IGP Food Web

To explore the effects of predation, competition, and hypoxia, three versions of the model were simulated under the high DO (normoxic) scenario and the low DO (hypoxic) scenarios for a total of six modeled conditions (Fig. 11.4). The first

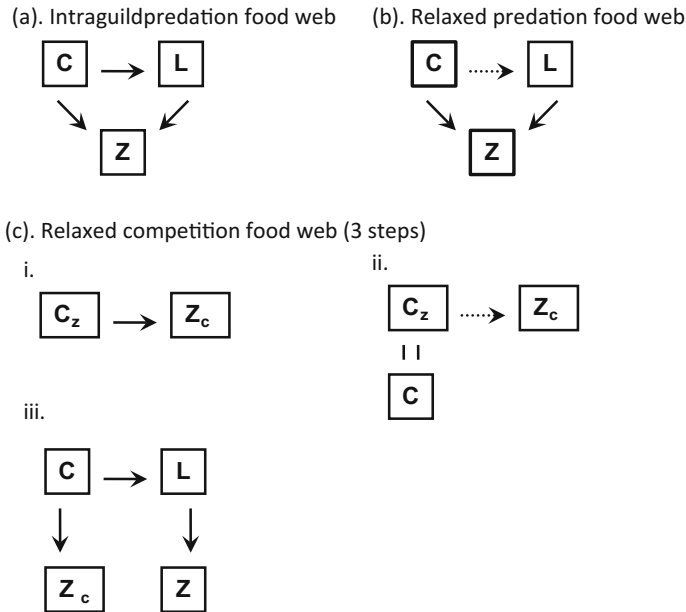


Fig. 11.4 Modeled simulations included three food webs, generated through five total iterations. **a** The baseline intra-guild predation (IGP) food web included ctenophores (C) as both predators on larval fish (L) and competitors for copepod prey (Z) (predation is designated by *solid arrows*), **b** the relaxed predation food web (RP) included ctenophore predation on larval fish, but larval fish were not removed from simulations (represented by a *dashed arrow*), and ctenophores and larval fish were competitors for copepod prey, and finally, **c** the relaxed competition food web (RC) had separate prey pools generated for ctenophores and larval fish through a series of steps. In the full RC food web, the zooplankton prey pool for ctenophores (Z_c) was generated from running simulations with a ctenophore-zooplankton-only model (i), a fitted density-independent model was run to calibrate ctenophores to baseline conditions (C) (ii), and the full RC model included two separate prey pools for ctenophore and larvae predators (Z_c and Z, respectively), with fitted ctenophores also preying on fish larvae (iii)

version of the model was the baseline version used in calibration and corroboration with the full predation and competitive interactions operating (Fig. 11.4a). The second version of the model relaxed the ctenophore predation effects on fish larvae (Fig. 11.4b). Ctenophore consumption depended on their encounters with fish larvae, but eaten larval fish were not removed from the simulation; therefore, ctenophores gained the appropriate prey resources, but fish larvae were not affected by ctenophore predation.

The third version of the model ultimately maintained the ctenophore predation effects on fish larvae, but relaxed the competition between ctenophores and fish larvae for copepods. Through a series of intermediate food webs, we created two sets of copepod densities (by stage, layer, and time step), one for ctenophores and

one for fish larvae, to allow ctenophores to eat larvae and zooplankton, while larvae experienced a separate zooplankton prey pool (Fig. 11.4c). First, the baseline model was run with only ctenophores and copepods, and the predicted copepod numbers by life stage, layer, and time step were recorded (Fig. 11.4c.i.). We then used these copepod densities as input back into the ctenophore-copepod-only model but without ctenophore effects on copepods, and recalibrated the ctenophore egg and larval mortality rates ($0.67\text{--}0.9 (12 \text{ h})^{-1}$; $0.74\text{--}0.9 (12 \text{ h})^{-1}$), so their dynamics closely resembled the baseline IGP version with the full interactions (Fig. 11.4c.ii.). Finally, using the recalibrated mortality rates, we ran the full model with ctenophores only preying upon their own pool of copepods (the output from ctenophore-copepod model) and fish larvae consuming their own pool of copepods (Fig. 11.4c.iii.). In this relaxed competition version, ctenophore dynamics resembled the dynamics in the IGP baseline with their consumption affecting fish larvae mortality, but their consumption of copepods not affecting the availability of copepods to fish larvae.

We first examined the baseline food web under both high and low DO conditions for general model behavior beyond the calibration and corroboration checks and for the effects of low DO on model dynamics. Second, we compared the predicted larval fish survival and growth among the three food webs for the high DO condition to determine the importance of ctenophore predation versus ctenophore competition on larval fish survival and growth. The third comparison was among the three food webs for high DO versus low DO to determine whether low DO altered the importance of predation versus competition obtained under high DO in the second comparison.

Model output variables averaged over the five replicate simulations include: (1) number of fish larvae surviving and their average duration from first feeding (i.e., introduced as model individuals) to 15 mm, and (2) percent survival of fish from egg to hatch, hatch to first feeding, first feeding to 15 mm, and egg to 15 mm. For simplicity and because of consistency among replicates, we used a single replicate simulation for each of the six conditions and examined for every 12-h time step over the 100 d of simulation: larval lengths and ctenophore weights over time for selected model individuals (every 50th model individual), and time series plots of larval, ctenophore, and adult-stage copepod densities by water layer. We also report water column integrated densities (i.e., sum of all individuals divided by volume of water column); these were output daily, and then the 100 values summarized as the minimum, average (\pm SE), and maximum values. Diets of ctenophores and larval fish (broken down by small (>5 mm), medium (5–10 mm), and large sized (>15 mm)) were summarized as the averaged proportion by biomass of nauplii, copepodites, and adult copepods over a single replicate simulation. Finally, as an aid for interpreting model results, we computed the average vertical overlap between ctenophores and fish larvae, ctenophores and copepods, and fish larvae and copepods for the duration of a single replicate simulation.

11.4 Results and Discussion

11.4.1 Model Calibration and Corroboration

We examined how DO could interact with food web structure to affect larval fish survival and growth. While both DO and food web structure altered outcomes for modeled larval fish, the effect of DO was not substantially altered under the three different food webs tested. Our IGP food webs included: baseline in which all predation and competitive interactions were operating, a version with relaxed competition between ctenophores and fish for zooplankton, and a version with relaxed predation of ctenophores on fish larvae. The ctenophore-fish larvae-copepod food web in this model typifies Chesapeake Bay and other temperate estuaries, and differs from more frequently examined IGP food webs in that the IGP predator (the ctenophore, *Mnemiopsis leidyi*) is also a superior competitor to its prey (fish larvae).

Using the calibrated parameter values, average larval growth rates in both the high and low DO baseline IGP food web model were similar to bay anchovy growth rates reported from field studies. Average growth rates of larval fish surviving to 15 mm in the baseline IGP food web model were 0.46 mm d⁻¹ at high DO and 0.61 mm d⁻¹ at low DO. Rilling and Houde (1999) reported field growth rates of larval bay anchovy ranging from 0.53 to 0.78 mm d⁻¹, and bay anchovy larvae from North Carolina were estimated to grow at about 4% d⁻¹ or equal to about 0.48 mm d⁻¹ (Fives et al. 1986).

Modeled ctenophore lengths and ctenophore egg production remained within the bounds observed in field samples and laboratory studies. Simulated ctenophore lengths under high and low DO ranged over the summer from 20 to 92 mm, the maximum being slightly smaller than the largest ctenophore length (100 mm) observed in the Chesapeake Bay system. Ctenophore egg production averaged about 1000 eggs ctenophore⁻¹ d⁻¹ (range of 0–11,360), which was similar to the range of 0–14,000 eggs ctenophore⁻¹ d⁻¹ reported in Purcell et al. (2001).

Simulated summertime densities of ctenophores and fish eggs and larvae were similar to values reported for Chesapeake Bay and the Patuxent River (Table 11.3). Simulated ctenophore densities averaged about 3.8 individuals m⁻³ over the summer (with a maximum daily value of 8.7), compared to summertime means of 0.03 to 6.83 in the Patuxent and 2.8 to 12.7 in the mainstem Chesapeake Bay. Averaged fish egg densities in the baseline simulations were about 2.5 eggs m⁻³, with a daily maximum of 20, while field data showed a range of summertime means of 0 to 41.3 in the Patuxent and 1.2 to 28.8 in the Chesapeake Bay. Simulated fish larval densities were also within the range of the field data; model averaged values were about 1.5 individuals m⁻³ for both yolk sac and feeding larvae in high DO and about 0.6 individuals m⁻³ in low DO, versus 1.6 to 12.9 for yolk sac and feeding larvae combined in the Patuxent and 0.3 to 3.3 in the Chesapeake Bay.

Simulated copepodite and adult copepod densities were similar to those reported for the Patuxent River estuary, while simulated copepod nauplii densities were

higher than reported values. Simulated values of copepodite and adult copepod densities averaged 106,000 individuals m^{-3} and 63,000 in high DO (summed value of about 160,000) and 87,000 and 49,000 in low DO (summed value of about 140,000), which were reasonable given the relatively wide range of summed observed values of 700–295,000 in the Patuxent and 800–75,000 in the Chesapeake Bay.

Simulated nauplii densities were almost 10 times higher than reported densities (Table 11.3). Simulated nauplii densities were 226,900 individuals m^{-3} under high DO and 190,800 individuals m^{-3} under low DO, while reported mean densities were less than 36,000. This is likely a combination of simulated densities being too high and field samples being underestimates due to difficulties in accurately sampling nauplii based on their small size and high variability. In other studies, nauplii densities of 100,000 individuals m^{-3} in the surface layer were reported for both the Patuxent River estuary (Heinle 1966) and the Chesapeake Bay (Purcell et al. 1994b), and Purcell et al. (1994b) even reported occurrences of copepodite and adult copepod densities approaching 100,000 individuals m^{-3} at some stations in August (implying nauplii densities were even higher). However, while these high densities occurred, they were extreme values rather than averaged values. Both simulated and observed copepods (Purcell et al. 1994b) were at their lowest densities during the summer period.

11.4.2 Baseline Model Behavior Under High DO

Ctenophore densities peaked during mid-summer coincident with the time that larval fish densities and zooplankton densities showed depressed values. Ctenophores peaked between days 180 and 200 at a water column integrated average density of about 9.0 individuals m^{-3} , and with most individuals in the bottom layer and secondarily in the pycnocline layer, more so during the day than at night (Fig. 11.5a). Larval fish densities reached their peak early in the summer (column integrated density of 6.0 individuals m^{-3}), as larval fish numbers accumulated from frequent spawning (Fig. 11.6a). Larval fish densities then declined during the middle of the summer and rebounded with a second, lower peak near the end of the summer. In the absence of ctenophore predation, a peak in density of larval fish would be expected in the middle of the summer, as a result of the build-up of repeated spawning events and removal of individuals as they reached 15 mm. Larval fish were spread between the bottom and pycnocline layers, with few larvae occurring in the surface layer at any time (Fig. 11.6a). Adult copepod densities showed a minimum during the mid-summer (2,000 individuals m^{-3} relative to an equilibrium value of 10,000), with high densities in the surface layer during the day and in the pycnocline during the nighttime (Fig. 11.7a). Nauplii and copepodites (not shown) had very similar temporal patterns as adult copepods.

Fish survival was low during the first feeding to 15-mm stage relative to egg and yolk sac larval stages due to ctenophore predation and extended exposure to

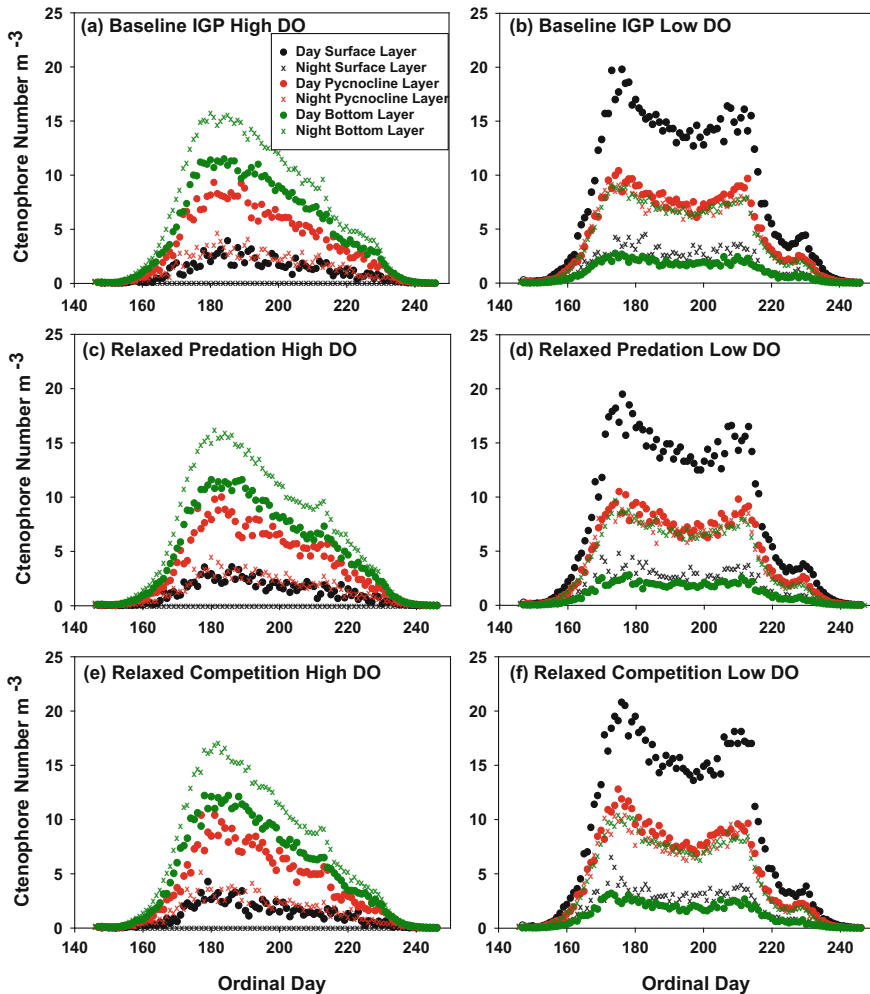


Fig. 11.5 Ctenophore number m^{-3} by layer plotted against ordinal day during both day (●) and night (x) for a representative simulation for each of six different food webs: **a** baseline IGP high DO, **b** baseline IGP low DO, **c** relaxed predation high DO, **d** relaxed predation low DO, **e** relaxed competition high DO, **f** relaxed competition low DO. *Black dots* denote the surface layer, *red dots* the pycnocline, and *green dots* the bottom layer

predation because of the long stage duration. Averaged survival (over the five replicate simulations) from egg production to hatching was 40%, hatch to first feeding was 16.8%, and first feeding to 15 mm was 2.1%, resulting in cumulative cohort survival of 0.14% and an average of 14.1 survivors to 15 mm (Table 11.4). First feeding to 15 mm survival due to constant mortality only (i.e., not from ctenophores and there was no DO-related mortality) was 20% (26 days at 3% per

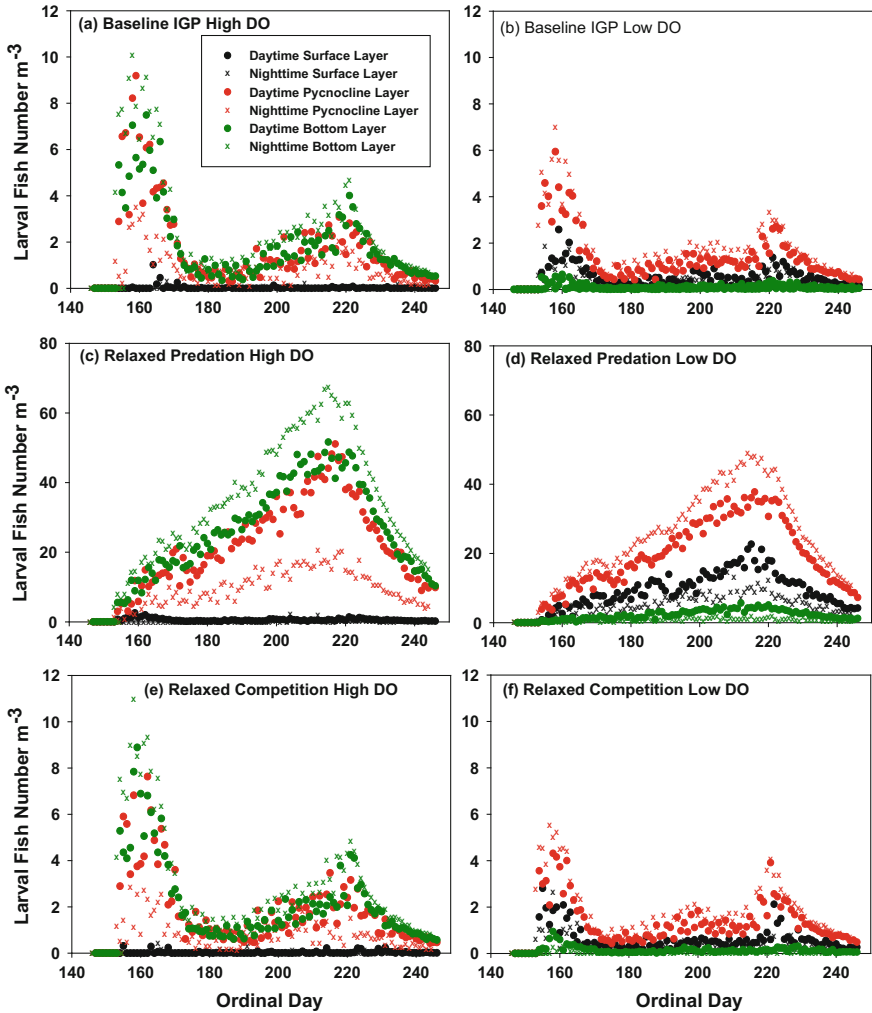


Fig. 11.6 Fish larvae number m^{-3} by layer plotted against ordinal day during both day (●) and night (x) for a representative simulation for each of six different food webs: **a** baseline IGP high DO, **b** baseline IGP low DO, **c** relaxed predation high DO, **d** relaxed predation low DO, **e** relaxed competition high DO, **f** relaxed competition low DO. *Black line* denotes the surface layer, *red line* the pycnocline, and *green line* the bottom layer. Note different scales

12 h, $0.97^{26 \cdot 2}$); thus, ctenophore predation reduced larval survival by an order of magnitude from 20 to 2.1%.

Ctenophore predation was very important to the survival of early life stages of fish in our modeled food webs. Movement in our model resulted in high overlap between ctenophores and larval fish, especially in food webs at high DO. The high consumption rates of ctenophores, coupled with their potential for rapid increase in

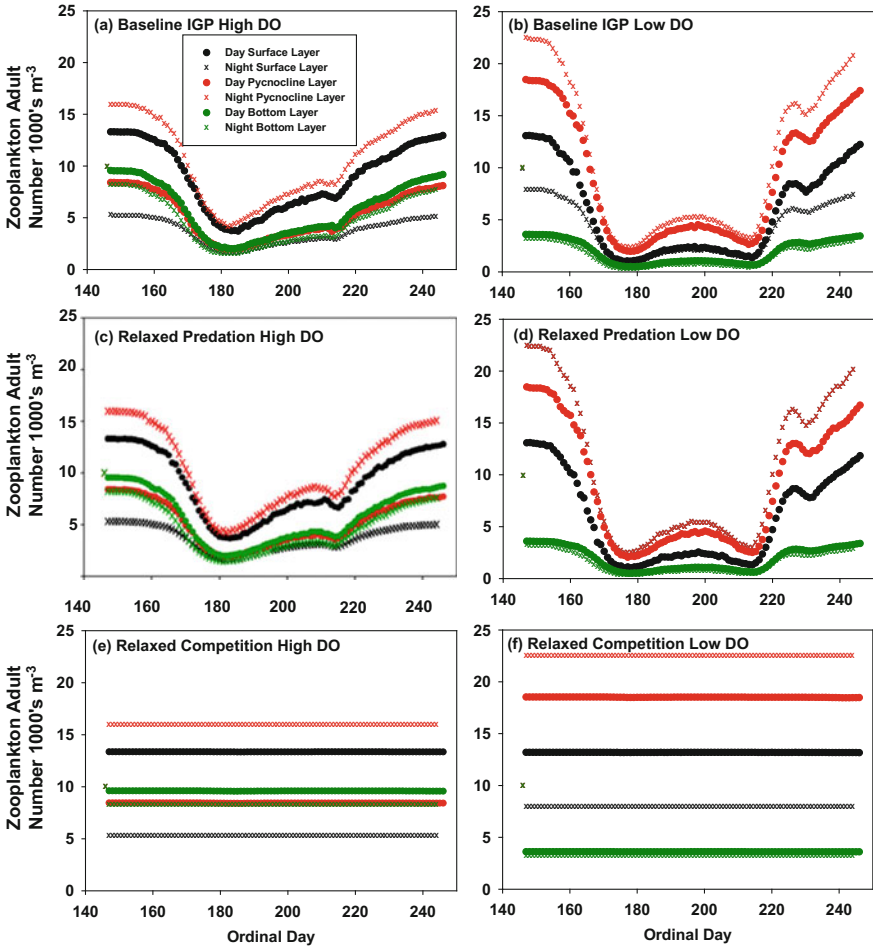


Fig. 11.7 Copepod number m^{-3} by layer plotted against ordinal day for the adult life stage during both day (●) and night (x) for a representative simulation for each of six different food webs: **a** baseline IGP high DO, **b** baseline IGP low DO, **c** relaxed predation high DO, **d** relaxed predation low DO, **e** relaxed competition high DO, **f** relaxed competition low DO. *Black dots* denote the surface layer, *red dots* the pycnocline, and *green dots* the bottom layer. Mean densities of copepodites and nauplii are reported for the baseline IGP food web (Table 11.6) and distribution patterns are similar to those of adult copepods in all food web scenarios. Single dots on the first day of simulations are an artifact of the initial density

biomass, makes them voracious planktonic predators (Monteleone and Duguay 1988; Purcell and Decker 2005). Predation is thought to be the largest source of mortality for the early life stages of fish (Bailey and Houde 1989). Slower growing larval fish are vulnerable to size-specific predation longer than are faster growing

Table 11.4 Results from five replicate runs of model simulations in the baseline IGP, relaxed predation, and relaxed competition food webs at both high and low DO. Reported values are the mean, minimum, and maximum total number of fish larvae reaching 15 mm and mean, minimum, and maximum total number of days for fish larvae to reach 15 mm during the 100 d simulation. No fish larvae less than 15 mm remain at the end of the simulations. Survivals are reported as percents. Minimum and maximum values based on the five replicate simulations are shown in parentheses for number of survivors to 15 mm and for larval duration

Variable	Baseline		Relaxed predation		Relaxed competition	
	High DO	Low DO	High DO	Low DO	High DO	Low DO
Number of survivors to 15 mm	14.1 (13.8–14.5)	9.9 (9.7–10.2)	352.0 (349.9–354.0)	243.5 (238.8–246.9)	41.5 (38.1–44.8)	19.4 (14.6–24.4)
Larval duration (days)	26.0 (25.5–26.4)	19.7 (19.3–20.1)	30.2 (30.1–30.4)	23.9 (23.7–24.3)	19.0 (18.9–19.0)	15.6 (15.4–15.9)
Egg to hatch survival	40.0	13.0	50.0	23.0	40.0	13.0
Hatch to first feeding survival	16.8	17.2	50.0	48.0	16.3	18.8
First feeding to 15 mm survival	2.1	4.4	14.2	22.2	6.4	7.7
Egg to 15 mm survival	0.14	0.098	3.55	2.45	0.417	0.189

larval fish (Bailey and Houde 1989). These model results support the importance of ctenophore predation to the survival of early life stages of fish suggested by experimental and field studies (Cowan and Houde 1993; Purcell et al. 1994a, b).

Larval fish growth rate (inversely related to duration) in the baseline model under high DO was affected indirectly via competition with ctenophores for copepod prey. Average larval growth rate to 15 mm was 0.46 mm d^{-1} , which corresponded to an average duration of 26 days from first feeding to 15 mm (Table 11.4). In general, larval fish lengths during the middle of the summer did not increase as rapidly as larval fish lengths during the early and late portions of the simulation (Fig. 11.8a). Slowed growth was due to competition and coincided with low copepod densities (Fig. 11.7a) and high ctenophore densities (Fig. 11.6a).

Larval fish diets in the baseline simulation were composed mostly of copepodites, with smaller proportions of copepod nauplii and adults (Table 11.5). The model restricted diets of small larvae (<5 mm) to nauplii; medium-sized larvae (5–10 mm) included copepodites, and large-sized larvae (>10 mm) further added adult copepods to their diet.

Growth of smaller ctenophores (<400 mg dw) was slowed during the middle summer by lowered copepod densities, while once ctenophores reached 400 mg dw, their growth rate was rapid throughout the summer (Fig. 11.9a). Ctenophores consumed mostly nauplii (Table 11.6). Weights of smaller ctenophores increased

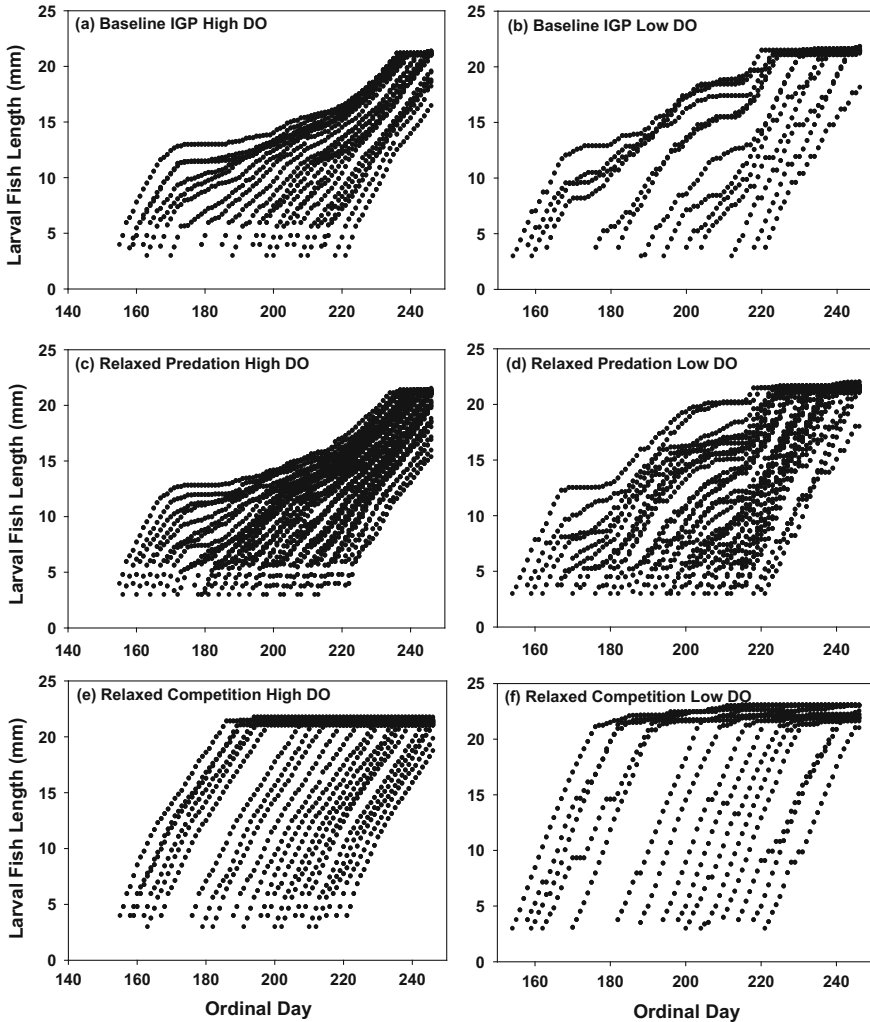


Fig. 11.8 Larval fish length (mm) plotted against ordinal day for six different simulations: **a** baseline IGP high DO, **b** baseline IGP low DO, **c** relaxed predation high DO, **d** relaxed predation low DO, **e** relaxed competition high DO, **f** relaxed competition low DO. Each *line* represents a cohort of individual feeding fish larvae throughout the simulation with each cohort entering the model at a different time step. The trajectory of size through time provides a representation of larval fish growth rates

rapidly early and late in the summer when nauplii densities were relatively high and showed slowed growth during the middle of the summer (days 50–150, Fig. 11.9a) when nauplii densities were low (Fig. 11.7a).

Table 11.5 Values for the mean proportion of biomass (mg dw) of each copepod life stage in modeled larval fish diets for three size classes of larval fish. Larval fish size classes were small (larval fish length <5 mm), medium (10 mm ≥ larval fish length ≥ 5 mm), and large (larval fish length >10 mm) for all three food webs: baseline IGP, relaxed predation, and relaxed competition at both high and low DO

	Small larvae		Medium larvae		Large larvae	
	High DO	Low DO	High DO	Low DO	High DO	Low DO
Baseline						
Copepod nauplii	1.00	1.00	0.13	0.36	0.26	0.38
Copepodites	0.00	0.00	0.87	0.64	0.60	0.35
Adult copepods	0.00	0.00	0.00	0.00	0.14	0.27
Relaxed predation						
Copepod nauplii	1.00	1.00	0.15	0.35	0.26	0.44
Copepodites	0.00	0.00	0.85	0.65	0.59	0.34
Adult copepods	0.00	0.00	0.00	0.00	0.15	0.22
Relaxed competition						
Copepod nauplii	1.00	1.00	0.26	0.88	0.32	0.49
Copepodites	0.00	0.00	0.74	0.12	0.25	0.15
Adult copepods	0.00	0.00	0.00	0.00	0.43	0.36

11.4.3 Effect of Low DO in the Baseline Food Web

Low DO caused a 30% reduction in overall survival of fish (9.9 vs. 14.1 survivors, Table 11.4), with the effect of DO on decreased egg survival partially offset by increased larval survival. Survival of fish eggs to hatch was lower in the low DO simulations than in high DO due to direct DO mortality on eggs. Thirteen percent of spawned fish eggs hatched to reach the yolk sac larvae stage at low DO as compared to 40% survival at high DO. Percent survival from hatch to first feeding was similar under both high and low DO (16.0 and 17.2%). In contrast, survival of larval fish from first feeding to 15 mm was higher under low DO (4.4% vs. 2.1%).

Higher larval fish survival under low DO was due to the effects of low DO reducing the overlap between fish larvae and ctenophores and the resulting reduction in encounter rates and predation mortality (two leftmost set of bars in Fig. 11.10). Potential encounter rates of later survivors were also reduced due to the higher mortality of fish eggs under hypoxia. The temporal patterns of densities between the low and high DO simulations were similar for ctenophores (Fig. 11.5a vs. b), larval fish (Fig. 11.6a vs. b), and adult copepod densities (Fig. 11.7a vs. b); however, the spatial overlap among the three vertical layers was altered. Peak densities of ctenophores shifted from the bottom and pycnocline layers under high DO (green in Fig. 11.5a) to the pycnocline and especially the surface layer during

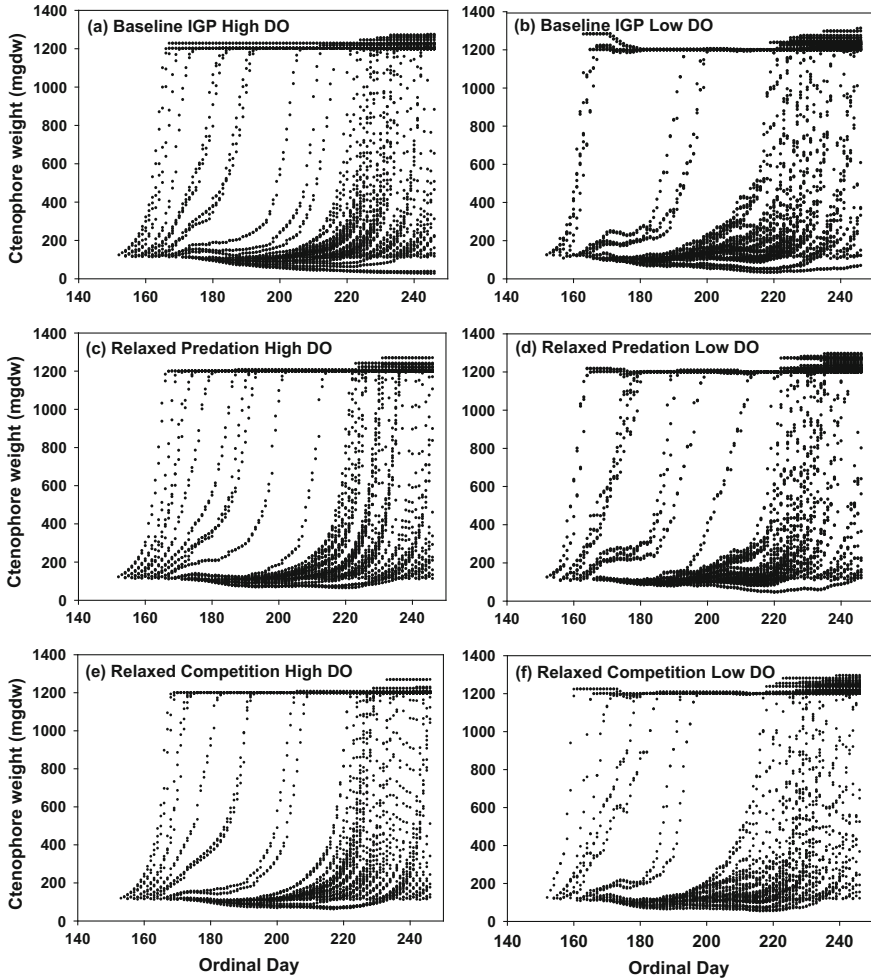


Fig. 11.9 Ctenophore weight (mg dw) plotted against ordinal day for six different simulations: **a** baseline IGP high DO, **b** baseline IGP low DO, **c** relaxed predation high DO, **d** relaxed predation low DO, **e** relaxed competition high DO, **f** relaxed competition low DO. Each line represents a cohort of individual ctenophores throughout the simulation with each cohort entering the model at a different time step. The trajectory of weight through time provides a representation of ctenophore growth rates

the day (black and red in Fig. 11.5b). Larval densities, which were highest in the bottom and pycnocline layers at high DO shifted mostly to the pycnocline (but not surface) layers (red in Fig. 11.6b). This resulted in the overlap between ctenophores and fish larvae being lowered from about 0.9 under high DO to about 0.5 under low DO (two leftmost bars in Fig. 11.10), resulting in reduced encounter rates and less predation by ctenophores on larval fish.

Table 11.6 Mean proportion of biomass (mg dw) due to each copepod life stage in ctenophore diets for the baseline, relaxed predation, and relaxed competition under both high and low DO scenarios. Copepods comprise the majority of ctenophore diets during the 100 d model simulation

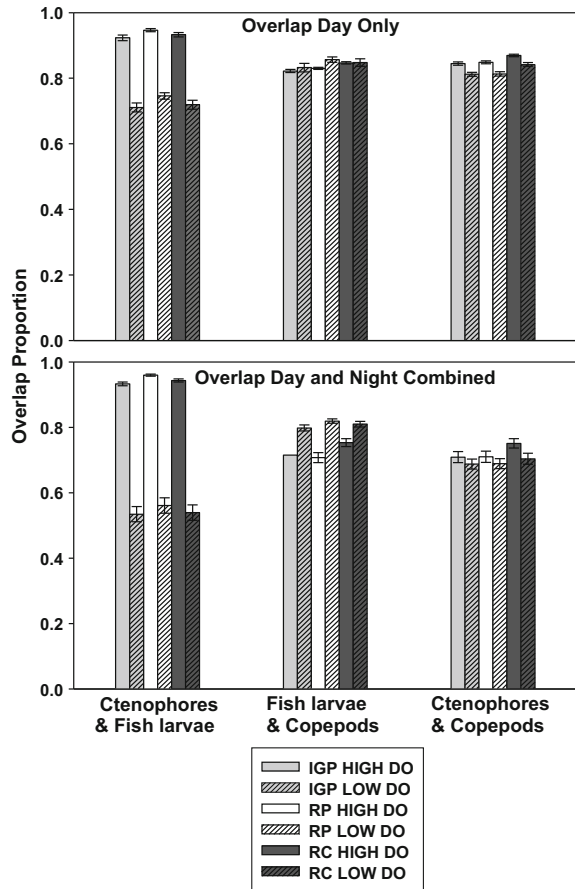
	High DO	Low DO
Baseline		
Copepod nauplii	0.78	0.81
Copepodites	0.08	0.07
Adult copepods	0.14	0.12
Relaxed predation		
Copepod nauplii	0.78	0.81
Copepodites	0.07	0.07
Adult copepods	0.14	0.12
Relaxed competition		
Copepod nauplii	0.78	0.81
Copepodites	0.08	0.07
Adult copepods	0.14	0.12

It was important to include a spatial component in the model because changes in vertical distribution in response to low DO triggered indirect effects. Spatial dynamics increases model complexity (Polis and Strong 1996), but including a spatial component can capture important features of food web interactions such as habitat refuges that increase food web persistence and reduce the likelihood of local extinctions (Keitt 1997; Fulton et al. 2004; Amarasekare 2007). Although larval fish survival decreased with low DO in all food webs, the response was not solely due to higher DO-related mortality. At low DO, larval survival from first feeding to 15 mm increased, and larval growth rate increased. Thus, even within a limited part of the life cycle (eggs and larvae), the response of fish to low DO can be complicated and include indirect effects mediated by changes in spatial overlaps with other members of the food web.

Larval fish growth rates were faster in the low DO simulation than in the high DO simulation, despite the negative direct effect imposed (Eq. 11.11), resulting in shorter larval stage duration (Table 11.4). Growth rates of fish larvae from first feeding to 15 mm was 0.61 mm d^{-1} in the low DO simulation, which corresponded to an average duration of 19.7 days, more than 6 days faster than the 26.0 days in the high DO baseline food web. Lowered larval fish densities due to increased egg mortality relaxed some of the predation pressure on copepods, and low DO caused slightly more overlap between larvae and copepods (middle set of bars in Fig. 11.10), resulting in faster growth for the remaining larvae. Reduced overlap between ctenophore predators and copepod prey at low DO also increased zooplankton prey densities available to larval fish.

Low DO caused a shift in larval fish diets away from copepodites (Table 11.5), but had no effect on ctenophore diets (Table 11.6). Small larval fish (length <5 mm) ate only copepod nauplii, so diets shifts due to low DO were not possible. Medium-sized larvae (5–10 mm) shifted to more nauplii, and large-size larvae shifted to more nauplii and more adult copepods in lower DO regions. Low DO did

Fig. 11.10 Vertical habitat overlap for three predator–prey pairs in the six different simulations: baseline intra-guild predation high DO (IGP HI DO, *gray bars*), baseline IGP low DO (IGP LO DO, *gray striped bars*), relaxed predation high DO (RP HI DO, *white bars*), relaxed predation low DO (RP LO DO, *white striped bars*), relaxed competition high DO (RC HI DO, *dark gray bars*), relaxed competition low DO (RC LO DO, *dark gray striped bars*). The three predator–prey pairs are: ctenophores and fish larvae, fish larvae and copepods, and ctenophores and copepods. Overlap for all three copepod life stages (copepod nauplii, copepodites, and adult copepods) was combined since their vertical habitat distribution was the same. Daytime values are shown for larval fish predation and day and night combined are shown for ctenophores predators. Data are mean overlap \pm 95% confidence interval



not affect the relative proportions of the three copepod life stages in ctenophore diets (Table 11.6).

Uncoupling the influence of a heterogeneous habitat from predation can be difficult (Anholt and Werner 1995). Spatial distributions of predators, competitors, and prey in the environment may be important for food web persistence and species coexistence (Rosenheim et al. 2004), with habitat complexity leading to food web complexity (Angel and Ojeda 2001). For example, the presence of a motile, omnivorous predator such as a ctenophore may stabilize complex food webs by increasing energy flow through weak links that promote species coexistence (McCann et al. 2005; Morris 2005). Under this premise, we attribute enhanced growth of larval fish in our modeled low DO food webs to greater spatial overlap of the larvae with copepod prey. But overall survival of larval fish cannot be explained by the same mechanism.

11.4.4 Importance of Predation Versus Competition to Fish Larvae Under High DO

Ctenophore predation had a much larger effect on larval fish survival than competition, and competition had a larger effect on larval growth; however, both predation and competition affected larval survival and growth. Under high DO conditions, survival of fish eggs to hatch increased from 40% in the baseline and relaxed competition food webs to 50% in the relaxed predation food web, hatch to first feeding survival increased from 16.8 to 50%, and first feeding to 15 mm survival increased from less than 6.4 to 14.2% (Table 11.4). Cumulative survival from egg to 15 mm was 24 times higher than baseline survival under relaxed predation (3.55/0.14), but only three times higher than baseline under relaxed competition (0.417/0.14).

Larval fish growth rates under high DO conditions were fastest in the relaxed competition food web and, due to less predation resulting in higher larval densities and increased density-dependent effects, slowest in the relaxed predation food web (Table 11.4). Larval duration was 7 days shorter than baseline when competition was relaxed and 4 days longer when predation was relaxed. Corresponding average growth rates of survivors were 0.63 mm d⁻¹ under relaxed competition, 0.46 mm d⁻¹ under baseline, and 0.40 mm d⁻¹ under relaxed predation. The slopes of lines for larval fish length versus day, an indication of growth rates, were very high throughout the relaxed competition food web (Fig. 11.8e), corresponding to high copepod densities throughout the summer (Fig. 11.7e). Slopes under baseline and relaxed predation flattened during mid-summer (Fig. 11.8a, c), which was when ctenophore densities were high (Fig. 11.6a, c) and copepod densities were low (Fig. 11.7a, c). Relaxed competition resulted in a shift of large-sized larvae to eat more adult copepods (Table 11.5). But the faster growth under relaxed competition resulted in a much smaller increase in survival than the relaxed predation scenario (Table 11.4).

Temporal patterns of larval densities showed a peak in mid-summer under relaxed predation (Fig. 11.6c), rather than a depression in mid-summer under baseline and relaxed competition (Fig. 11.6a, e). Water column integrated peak densities were 40 individuals m⁻³ under relaxed predation compared to less than 6 individuals m⁻³ in both baseline and relaxed competition. Relaxed predation and relaxed competition did not alter the vertical distribution of the larvae, with most larvae in the bottom and pycnocline layers as in baseline (red and green in Fig. 11.6 a, c, e). Thus, the drop in mid-summer larval densities under baseline was due to predation effects, rather than competition for zooplankton leading to slowed growth of larvae, longer duration, and higher cumulative mortality.

Ctenophores were generally unaffected by the relaxed competition and predation food webs. The magnitude and temporal pattern of ctenophore densities (Fig. 11.5a, c, e), growth rates (Fig. 11.9a, c, e), and diets (Table 11.6) were similar under high DO in all three food webs.

11.4.5 Interaction of Low DO with Different Predation and Competition Conditions

We used a factorial design in model simulations to isolate the interaction effect between DO level and food web type and found little evidence of an interaction effect. The effects of high versus low DO on larval survival and growth was consistent across the three food webs (Table 11.4), suggesting that there was not a strong interaction between DO conditions and food web type. The only exception was that DO had a larger effect on larval survival in the relaxed competition food web compared to the other food webs. Survival from egg to 15 mm under relaxed predation was 3.55% under high DO and 2.45% under low DO (a 31% decrease), which was very similar to the decrease under baseline (0.14% vs. 0.098%, or a 30% decrease). However, under relaxed competition, survival under high DO was 0.417% vs. 0.189%, or a 54% decrease, compared to a 30% decrease in survival under baseline. The difference was that first feeding to 15 mm survival increased much less (and therefore offset less of the increased egg mortality) under relaxed competition (6.4 to 7.7%), than the more than doubling under baseline (2.1 to 4.4%) and the 50% increase (14.2% to 22.2%) under relaxed predation (Table 11.4). The temporal pattern of larval densities, while different in the relaxed predation food web, all showed similar general reductions in densities from high to low DO and a shift from the bottom layer to the pycnocline and surface layers (Fig. 11.6a vs. b, c vs. d, e vs. f).

Going from high to low DO also had a consistent effect on larval growth and diets across the three food webs. Larval durations were 18–24% shorter at low DO compared to high DO for all three food webs (Table 11.4). Larval lengths over time showed consistently steeper slopes (faster growth and shorter duration) during the mid-summer under low DO (Fig. 11.8a vs. b, c vs. d, e vs. f). As with going from high to low DO under baseline, diets of the medium-sized larvae shifted away from copepodites toward nauplii and diets of large-sized larvae shifted to greater consumption of nauplii and adult copepods (Table 11.5).

Low DO affected ctenophore densities, growth, and diets similarly in all three food webs. Water column ctenophore densities peaked at around 9 individuals m^{-3} under high DO in the three food webs and at about 8 individuals m^{-3} in the low DO food webs and showed similar shifts by layer (Fig. 11.5). Ctenophore growth was also similarly slowed under low DO for all three food webs (Fig. 11.9). Ctenophore diets were very similar across all food webs and for low and high DO conditions (Table 11.6).

DO also had only small effects on the relative importance of competition versus predation to larval survival and growth (Table 11.4). The increase in larval survival from baseline to relaxed predation was the same for high DO (0.14 to 3.55%, 25x higher) as for low DO (0.098 to 2.45%, 25x higher). Similarly, the increase in larval survival was similar for baseline to relaxed competition for high DO (0.417/0.14, or 3x)

versus low DO (0.189/0.098, or 2x). Thus, the effect of DO (high vs. low) on larval survival and growth did not depend on the food web and DO did not greatly change the relative importance of competition versus predation within the food web.

The relaxed predation food web results showed that larval densities would peak in mid-summer but that the ctenophore predation in the baseline IGP food web and in the relaxed competition food web caused a mid-summer dip in larval densities. Note that model simulations were conducted without sea nettle predators, which can depress ctenophore densities in some field populations. Relaxing predation resulted in a 25x increase in larval survival, but relaxing competition resulted in the smaller but still important 3x increase in survival. Relaxing competition resulted in shorter larval stage durations, and relaxed predation (because of high larval densities) resulted in longer larval stage durations.

In our analysis, the DO effects were consistent across food webs and DO did not greatly affect the importance of competition versus predation. These results suggest that the effects of DO we found are robust and likely apply to a broad set of field situations. The two extreme food webs (competition completely relaxed; predation completely relaxed) bound the conditions observed in many estuaries and the differences in the food webs possible among spatial subregions and during different time periods within a system.

11.5 Conclusion

Intraguild predation food webs are thought to persist due to the superiority of the IGP prey in exploiting shared resources, or because IGP prey has a resource subsidy unavailable to the IG predator (Polis 1984). But in our modeled food web, and in the Chesapeake Bay system, ctenophores were both a predator on fish larvae and a superior competitor for copepod prey. Our result, of lowest survival of early life stages of fish in the IGP food web, provides evidence that this particular IGP food web would likely not facilitate persistence of larval fish. However, the modeled system represents a subset of the complete food web structure of many temperate estuaries. Factors such as the age structure and seasonality of the food web, as well as the effects of DO on vertical habitat overlap, limit ctenophore predation on fish egg and larval stages to a brief period during the summer months. Temporal and spatial patchiness of ctenophores due to predation by *Chrysaora quinquecirrha* medusa, not considered in these simulations, can also contribute to larval fish survival in the field.

Using a modeling approach to address questions about food web structure and the effects of low DO on trophic interactions had advantages as well as limitations. The individual-based, spatially explicit food web model enabled us to simulate the effects of ctenophore predation and competition with fish larvae; the ability to

simulate competition was especially valuable because competition is difficult to isolate in either the field or laboratory. In constructing the food web model, we made certain simplifying assumptions (e.g., constant temperature, DO levels fixed through time, simple behavioral rules for feeding and movement) to keep a moderate level of simplicity in a complicated model. Next steps for the food web model could include adding more trophic levels for both prey (e.g., phytoplankton and microzooplankton) and predators (*Chrysaora quinquecirrha* medusae), and considering traits of larval fish other than bay anchovy to test whether our predictions are species specific or generally robust, and therefore applicable to other estuarine food webs. Myriad variations can include additional within-summer variation in environmental variables and in the phenologies of the zooplankton, ctenophores, and larval fish. Low DO is often associated with eutrophication, and additional simulations might include eutrophication effects on the food web. Our results demonstrate that our ability to assess hypoxia effects on fish is improved by models that allow for both indirect effects via the food web and alteration of spatial distributions.

Acknowledgements We thank W. Boynton, T. Miller, and J. Purcell for comments on a previous version of this manuscript and G. Waldbusser for assistance with figure preparation. Comments from two anonymous reviewers greatly improved this submission, and we are grateful for their efforts. Research was partially supported (KAR) by the National Oceanographic and Atmospheric Administration, Center for Sponsored Coastal Ocean Research (CSCOR) CHRP Grant numbers NA10NOS4780157 awarded to Louisiana State University and NA10NOS4780138 awarded to the Smithsonian Environmental Research Center (DLB). This is publication number 220 of the NOAA's CSCOR NGOMEX and CHRP programs.

Appendix A. Stage-Based Matrix Projection Models for Fish Eggs and Yolk Sac Larvae, and Ctenophore Eggs and Larvae

Six stage-based matrix projection models were used to update fish eggs and yolk sac larvae, and ctenophore eggs and larvae. There was a model for fish and for ctenophores for each of the three layers. The models were 2×2 and operated on a 12-h time step. For each model, we computed the diagonal and subdiagonal elements from stage survival and duration every 12 h. We first computed from survival over 12 h for the i th stage from specified daily instantaneous survival rates as $S_i = e^{-M_i/2}$. For fish eggs only, DO was used to compute *SurEggDO* (Eq. 11.13), and S_i for eggs was then adjusted as $S_i \cdot \text{SurEggDO}$. We then computed φ_i , survival for each time period, from S_i and duration (D_i , number of 12 h):

$$\varphi_i = \frac{S_i^D - S_i^{D-1}}{S_i^D - 1}$$

The diagonal and off-diagonal elements were then:

$$D_{i,i} = S_i \cdot (1 - \varphi_i)$$

$$D_{i,i+1} = S_i \cdot \varphi_i$$

Fecundity (usually the top row of the matrices) was dealt with by simply adding newly entering eggs to those already present in each layer every 12 h. Number of eggs added was computed based on day of year, and dynamically each 12 h for ctenophores based on growth and summed over individual ctenophores.

At the beginning of each 12-h time step, the matrices were specified and the numbers of individuals in each stage were updated. Newly entering eggs for fish and ctenophores were then added to their egg abundances. Then during the next 12 h, consumption of fish eggs and yolk sac larvae by ctenophores was subtracted from the total number of individuals in each layer. The decreased numbers of individuals in each life stage in each layer were then used to start the next time step.

The mortality rates, durations, and fecundity rates are shown in Table 11.7. Typical matrices for each of the taxa were:

Fish:

$$\begin{bmatrix} 0.75 & 5 \\ 0.25 & 0.75 \end{bmatrix}$$

Ctenophores:

$$\begin{bmatrix} 0.402 & 20 \\ 0.27 & 0.402 \end{bmatrix}$$

Table 11.7 Mortality, stage duration, and fecundity rates for stage-based matrix projection models for fish eggs and yolk sac larvae, and ctenophore eggs and larvae

Taxa	Stages	Duration (12 h)	Mortality (d ⁻¹)	Fecundity (entering) or exiting
Fish	Eggs	2.0	0.001	Added by layer as 100 eggs m ⁻³ ; every 3 days for days 150–189 and 213–220; daily for days 190–212
	Yolk sac larvae	4.0	0.001	Become individual feeding larvae
Ctenophores	Eggs	2.0	0.8	Added by layer by summing over eggs produced by individual ctenophores
	Larvae	20.0	0.6	Become lobates; then after 5–7 days became 25-mm individuals

References

- Adamack AT, Rose KA, Breitburg DL, Nice AJ, Lung WS (2012) Simulating the effects of hypoxia on bay anchovy egg and larval mortality in the Patuxent River using coupled watershed, water quality, and individual-based predation models. *Mar Ecol Prog Ser* 445:141–161
- Angel A, Ojeda FP (2001) Structure and trophic organization of subtidal fish assemblages on the northern Chilean coast: the effect of habitat complexity. *Mar Ecol Prog Ser* 217:81–91
- Amaraskare P (2007) Trade-offs, temporal variation, and species coexistence in communities with intraguild predation. *Ecology* 88:2720–2728
- Anholt BR, Werner EE (1995) Interaction between food availability and predation mortality mediated by adaptive behavior. *Ecology* 76:2230–2234
- Arim M, Marquet PA (2004) Intraguild predation: a widespread interaction related to species biology. *Ecol Lett* 7:557–564
- Bailey KM, Houde ED (1989) Predation on eggs and larvae of marine fishes and the recruitment problem. *Adv Mar Biol* 25:1–67
- Breitburg DL, Adamack A, Rose KA, Kolesar SE, Decker MB, Purcell JE, Keister JE, Cowan JH Jr (2003) The pattern and influence of low dissolved oxygen in the Patuxent River, a seasonally hypoxic estuary. *Estuaries* 26:280–297
- Breitburg DL, Craig JK, Fulford RS, Rose KA, Boynton WR, Brady DC, Ciotti BJ, Diaz RJ, Friedland KD, Hagy JD III, Hart DR, Hines AH, Houde ED, Kolesar SE, Nixon SW, Rice JA, Secor DH, Targett TE (2009) Nutrient enrichment and fisheries exploitation: interactive effects on estuarine living resources and their management. *Hydrobiologia* 629:31–47
- Breitburg DL, Loher T, Pacey CA, Gerstein A (1997) Varying effects of low dissolved oxygen on trophic interactions in an estuarine food web. *Ecol Monogr* 67:489–507
- Brownlee DC, Jacobs F (1987) Mesozooplankton and microzooplankton in the Chesapeake Bay. In: Majumdar SK, Hall LW, Austin HM (eds) Contaminant problems and management of living Chesapeake Bay resources. The Pennsylvania Academy of Science, Philadelphia, Pennsylvania, pp 217–269
- Caddy JF (1993) Toward a comparative evaluation of human impacts on fishery ecosystems of enclosed and semi-enclosed areas. *Rev Fish Sci* 1:57–95
- Cloern JE (2001) Our evolving conceptual model of the coastal eutrophication problem. *Mar Ecol Prog Ser* 210:223–253
- Cowan JH Jr, Houde ED (1993) Relative predation potentials of scyphomedusae, ctenophores and planktivorous fish on ichthyoplankton in Chesapeake Bay. *Mar Ecol Prog Ser* 95:55–65
- Cowan JH Jr, Rose KA, Houde ED, Wang SB, Young J (1999) Modeling effects of increased larval mortality on bay anchovy population dynamics in the mesohaline Chesapeake Bay: evidence for compensatory reserve. *Mar Ecol Prog Ser* 185:133–146
- Diaz RJ, Rosenberg R (2008) Spreading dead zones and consequences for marine ecosystems. *Science* 32:926–929
- Decker MB, Breitburg DL, Purcell JE (2004) effects of low dissolved oxygen on zooplankton predation by the ctenophore *Mnemiopsis leidyi*. *Mar Ecol Prog Ser* 280:163–172
- Diehl S (1995) Direct and indirect effects of omnivory in a littoral lake community. *Ecology* 76:1727–1740
- Diehl S, Feiel M (2000) Effects of enrichment on three-level food chains with omnivory. *Am Nat* 155:200–218
- Dorsey SE, Houde ED, Gamble JC (1996) Cohort abundances and daily variability in mortality of eggs and yolk-sac larvae of bay anchovy, *Anchoa mitchilli*, in Chesapeake Bay. *Fish Bull* 94:257–267
- Ehler LE (1996) Structure and impact of natural enemy guilds in biological control of insect pests. In: Polis GA, Winemiller KO (eds) Food webs: integration of patterns and dynamics. Chapman and Hall, New York, NY, pp 337–342

- Ekau W, Auel H, Pörtner H-O, Gilbert D (2010) Impacts of hypoxia on the structure and processes in pelagic communities (zooplankton, macro-invertebrates and fish). *Biogeosciences* 7:1669–1699
- Fagan WF (1997) Omnivory as a stabilizing feature of natural communities. *Am Nat* 150:554–567
- Fives JM, Warlen SM, Hoss DE (1986) Aging and growth of larval bay anchovy, *Anchoa mitchilli*, from the Newport River Estuary, North Carolina. *Estuaries* 9:362–367
- Fulton EA, Smith ADM, Johnson CR (2004) Effects of spatial resolution on the performance and interpretation of marine ecosystem models. *Ecol Model* 176:27–42
- Gerritsen J, Strickler JR (1977) Encounter probabilities and community structure in zooplankton: a mathematical model. *J Fish Res Board Can* 34:73–82
- Gilbert D, Rabalais NN, Díaz RJ, Zhang J (2010) Evidence for greater oxygen decline rates in the coastal ocean than in the open ocean. *Biogeosciences* 7:2283–2296
- Grove M, Breitburg DL (2005) Growth and reproduction of gelatinous zooplankton exposed to low dissolved oxygen. *Mar Ecol Prog Ser* 301:185–198
- Gurevitch J, Morrison JA, Hedges LV (2000) The interaction between competition and predation: a meta-analysis of field experiments. *Am Nat* 155:435–453
- Harris RP, Wiebe P, Lenz J, Skjoldal HR, Huntley, M (2000) ICES zooplankton methodology manual. Academic Press London, UK, 705 pps
- Heinle DR (1966) Production of a calanoid copepod, *Acartia tonsa*, in the Patuxent River estuary. *Chesap Sci* 7:59–74
- Heithaus MR (2001) Habitat selection by predators and prey in communities with asymmetrical intraguild predation. *Oikos* 92:542–554
- Holt RD, Polis GA (1997) A theoretical framework for intraguild predation. *Am Nat* 149:745–764
- Hunter JR, Leong R (1981) The spawning energetics of female Northern Anchovy, *Engraulis mordax*. *Fish Bull* 79:215–230
- Janssen A, Sabelis MW, Magalhães S, Montserrat M, van der Hammen T (2007) Habitat structure affects intraguild predation. *Ecology* 88:2713–2719
- Keister JE, Houde ED, Breitburg DL (2000) Effects of bottom-layer hypoxia on abundances and depth distribution of organisms in Patuxent River, Chesapeake Bay. *Mar Ecol Prog Ser* 205:43–59
- Keitt TH (1997) Stability and complexity on a lattice: coexistence of species in an individual-based food web model. *Ecol Model* 102:243–258
- Kemp WM, Boynton WR, Adolf JE, Boesch DF, Boicourt WC, Brush G, Cornwell JC et al (2005) Eutrophication of Chesapeake Bay: historical trends and ecological interactions. *Mar Ecol Prog Ser* 303:1–29
- Kidwell DM, Lewitus AJ, Jewett EB, Brandt S, Mason DM (2009) Ecological impacts of hypoxia on living resources. *J Exp Mar Biol Ecol* 381:S1–S3
- Kimmel DG, Roman MR (2004) Long-term trends in mesozooplankton abundance in Chesapeake Bay, USA: influence of freshwater input. *Mar Ecol Prog Ser* 267:71–83
- Kolesar, SE (2006) The effects of low dissolved oxygen on predation interactions between *Mnemiopsis leidyi* ctenophores and larval fish in the Chesapeake Bay ecosystem. PhD dissertation, University of Maryland, College Park, MD
- Kolesar SE, Breitburg DL, Purcell JE, Decker MB (2010) Effects of hypoxia on *Mnemiopsis leidyi*, ichthyoplankton and copepods: clearance rates and vertical habitat overlap. *Mar Ecol Prog Ser* 411:173–188
- Kremer P (1976) Population dynamics and ecological energetics of a pulsed zooplankton predator, the ctenophore *Mnemiopsis leidyi*. In: Wiley ML (ed) *Estuarine Processes*. Academic Press, NY, 1:197–215
- Kremer P (1979) Predation by the ctenophore *Mnemiopsis leidyi* in Narragansett Bay, Rhode Island. *Estuaries* 2:97–105
- Kremer P, Reeve MR (1989) Growth dynamics of a ctenophore (*Mnemiopsis*) in relation to variable food supply. II. Carbon budgets and growth model. *J Plankton Res* 11:535–552
- Kreps TA, Purcell JE, Heidelberg KB (1997) Escape of the ctenophore *Mnemiopsis leidyi* from the scyphomedusa predator *Chrysaora quinquecirrha*. *Mar Biol* 128:441–446

- Laurence GC (1976) Caloric values of some North Atlantic calanoid copepods. *Fish Bull* 74:218–220
- Levin LA, Ekau W, Gooday AJ, Jorissen F, Middelburg JJ, Naqvi SWA, Neira C, Rabalais NN, Zhang J (2010) Effects of natural and human-induced hypoxia on coastal benthos. *Biogeosciences* 6:2063–2098
- McCann K, Hastings A, Huxel GR (1998) Weak trophic interactions and the balance of nature. *Nature* 395:794–798
- McCann KS, Rasmussen JB, Umbanhowar J (2005) The dynamics of spatially coupled food webs. *Ecol Lett* 8:513–523
- Monteleone DM, Duguay LE (1988) Laboratory studies of predation by the ctenophore *Mnemiopsis leidyi* on the early stages in the life history of the bay anchovy, *Anchoa mitchilli*. *J Plankton Res* 10:359–372
- Morris DW (2005) Paradoxical avoidance of enriched habitats: have we failed to appreciate omnivores? *Ecology* 86:2568–2577
- Navarrette SA, Menge BA, Daley BA (2000) Species interactions in intertidal food webs: prey or predation regulation of intermediate predators? *Ecology* 81:2264–2277
- Polis GA (1984) Age structure component of niche width and intraspecific resource partitioning: can age groups function as ecological species? *Am Nat* 123:541–564
- Polis GA (1998) Stability is woven by complex webs. *Nature* 395:744–745
- Polis GA, Holt RD (1992) Intraguild predation: the dynamics of complex trophic interactions. *Trends Ecol Evol* 7:151–154
- Polis GA, Myers CA, Holt RD (1989) The ecology and evolution of intraguild predation: potential competitors that eat each other. *Annu Rev Ecol Syst* 20:297–330
- Polis GA, Strong DR (1996) Food web complexity and community dynamics. *Am Nat* 147:813–835
- Purcell JE, Arai MN (2001) Interactions of pelagic cnidarians and ctenophores with fish: a review. *Hydrobiologia* 451:27–44
- Purcell JE, Breitburg DL, Decker MB, Graham WM, Youngbluth MJ, Raskoff KA (2001) Pelagic cnidarians and ctenophores in low dissolved oxygen environments: a review. In: Rabalais NN, Turner RE (eds) Coastal hypoxia: consequences for living resources and ecosystems, vol 58. American Geophysical Union, Coastal and Estuarine Studies, pp 77–100
- Purcell JE, Decker MB (2005) Effects of climate on predation by ctenophores and scyphomedusae on copepods in Chesapeake Bay during 1987–2000. *Limnol Oceanogr* 50:376–387
- Purcell JE, Decker MB, Breitburg DL, Broughton KJ (2014) Fine-scale vertical distributions of *Mnemiopsis leidyi* ctenophores: predation on copepods relative to stratification and hypoxia. *Mar Ecol Prog Ser* 500:103–120
- Purcell JE, Nemazie DA, Dorsey SE, Houde ED, Gamble JC (1994a) Predation mortality of bay anchovy (*Anchoa mitchilli*) eggs and larvae due to scyphomedusae and ctenophores in Chesapeake Bay. *Mar Ecol Prog Ser* 114:47–58
- Purcell JE, White JR, Roman MR (1994b) Predation by gelatinous zooplankton and resource limitation as potential controls of *Acartia tonsa* copepod populations in Chesapeake Bay. *Limnol Oceanogr* 23:740–751
- Rabalais NN, Díaz RJ, Levin LA, Turner RE, Gilbert D, Zhang J (2010) Dynamics and distribution of natural and human-caused hypoxia. *Biogeosciences* 7:585–619
- Reeve MR, Syms MA, Kremer P (1989) Growth dynamics of a ctenophore (*Mnemiopsis*) in relation to variable food supply I. Carbon biomass, feeding, egg-production, growth and assimilation efficiency. *J Plankton Res* 11:535–552
- Rilling GC, Houde ED (1999) Regional and temporal variability in growth and mortality of bay anchovy, *Anchoa mitchilli*, larvae in Chesapeake Bay. *Fish Bull* 97:555–569
- Rose KA, Adamack AT, Murphy CA, Sable SE, Kolesar SE, Craig JK, Breitburg DL, Thomas P, Brouwer MH, Cerco CF, Diamond S (2009) Does hypoxia have population-level effects on coastal fish? Musings from the virtual world. *J Exp Mar Biol Ecol* 381:S188–S203

- Rose KA, Cowan JH Jr, Clark ME, Houde ED, Wang SB (1999) An individual-based model of bay anchovy population dynamics in the mesohaline region of Chesapeake Bay. *Mar Ecol Prog Ser* 185:113–132
- Rosenheim JA, Glik TE, Goeriz RE, Rämert B (2004) Linking a predator's foraging behavior with its effects on herbivore population suppression. *Ecology* 85:3362–3372
- Rosenheim JA (2007) Intraguild predation: new theoretical and empirical perspectives. *Ecology* 88:2679–2680
- Scheffer M, Baveco JM, DeAngelis DL, Rose KA, van Nes EH (1995) Super-individuals: a simple solution for modelling large populations on an individual basis. *Ecol Model* 80:161–170
- Snyder WE, Wise DH (2001) Contrasting trophic cascades generated by a community of generalist predators. *Ecology* 82:1571–1583
- Tester PA, Turner JT (1988) Comparative carbon-specific ingestion rates of phytoplankton by *Acartia tonsa*, *Centropages velificatus* and *Eucalanous pileatus* grazing on natural phytoplankton assemblages in the plume of the Mississippi River (northern Gulf of Mexico continental shelf). *Hydrobiologia* 167(168):211–217
- Thompson RM, Hemberg M, Starzomski BM, Shurin JB (2007) Trophic levels and trophic tangles: the prevalence of omnivory in real food webs. *Ecology* 88:612–617
- Tucker JW Jr (1989) Energy utilization in bay anchovy, *Anchoa mitchilli*, and black sea bass, *Centropristis striata striata*, eggs and larvae. *Fish Bull* 78:279–293
- Vandermeer J (2006) Omnivory and the stability of food webs. *J Theor Biol* 238:497–504
- Waggett R, Costello JH (1999) Capture mechanisms used by the lobate ctenophore, *Mnemiopsis leidyi*, preying on the copepod *Acartia tonsa*. *J Plankton Res* 21:2037–2052
- Wang SB, Houde ED (1994) Energy storage and dynamics in bay anchovy *Anchoa mitchilli*. *Mar Biol* 121:219–227
- Wissinger S (1992) Niche overlap and the potential for competition and intraguild predation between size-structured populations. *Ecology* 73:1431–1444
- Wissinger S, McGrady J (1993) Intraguild predation and competition between larval dragonflies: direct and indirect effects on shared prey. *Ecology* 74:207–218
- Zhang J, Gilbert D, Gooday AJ, Levin L, Naqvi SWA, Middelburg JJ, Scranton M, Ekau W, Peña A, Dewitte B, Oguz T, Monteiro PMS, Urban E, Rabalais NN, Ittekkot V, Kemp WM, Ulloa O, Elmgren R, Escobar-Briones E, Van der Plas AK (2010) Natural and human-induced hypoxia and consequences for coastal areas: synthesis and future development. *Biogeosciences* 7:1443–1467